

# Nonlinear Nonmodal Stability Theory

**R. R. Kerswell,**

School of Mathematics, Bristol University, Bristol, U.K., B8 1TW; email:  
R.R.Kerswell@bris.ac.uk

Xxxx. Xxx. Xxx. Xxx. YYYY. AA:1-30

This article's doi:  
10.1146/((please add article doi))

Copyright © YYYY by Annual Reviews.  
All rights reserved

## **Keywords**

transition, optimization, energy growth, nonlinear stability

## **Abstract**

This review discusses a recently developed optimization technique for analysing the nonlinear stability of a flow state. It is based upon a nonlinear extension of nonmodal analysis and, in its simplest form, consists of finding the disturbance to the flow state of a given amplitude which experiences the largest energy growth at a certain time later. When coupled with a search over the disturbance amplitude, this can reveal the disturbance of least amplitude - called the 'minimal seed' - for transition to turbulence. The approach bridges the theoretical gap between (linear) nonmodal theory and the (nonlinear) dynamical systems approach to fluid flows by providing the ability to explore phase space a finite distance from the reference flow state. Various ongoing and potential applications of the technique are discussed.

## 1. History and Motivation

Hydrodynamic stability theory has been of central importance in fluid mechanics ever since the observation that the property of a flow state being a solution of the governing equations is no guarantee that it will actually be realised in practice. Starting in the late 19th century and stimulated by the first controlled experiments of Reynolds (1883a,b), the initial attempts to rationalise why a flow state might be unstable centred on the idea of linear stability analysis (Rayleigh 1880, Kelvin 1887). In this, the linearised initial value problem describing how infinitesimal disturbances temporally evolve on top of the steady reference state is converted into an eigenvalue problem for the (possibly complex) growth rates of ‘normal’ modes whose temporal behaviour is exponential. These growth rates reveal the long time behaviour of the system, with just a single unstable one being enough to establish the linear instability of the reference state. The approach works well in explaining some experiments - for example, Rayleigh-Benard convection (Rayleigh 1916) and Taylor-Couette flow (Taylor 1923) - but not others, with wall-bounded shear flows such as plane Couette flow, channel flow and pipe flow being prime examples of failure.

Linear stability analysis, however, says nothing about the short-time behaviour of the linearised initial value problem which it was realised much later could be very different (Boberg & Brosa 1988, Farrell 1988, Gustavsson 1991, Butler & Farrell 1992, Reddy & Henningson 1993, Henningson & Reddy 1994, Trefethen et al. 1993; see Schmid 2007 for a review). A new formulation was developed to analyse this behaviour - variously called ‘transient growth’ (Reddy & Henningson 1993), ‘optimal perturbation theory’ (Butler & Farrell 1992) or ‘nonmodal analysis’ (Schmid 2007) - which started to explain the ‘hit-or-miss’ performance of linear stability analysis by revealing that for flows with no predicted long-time disturbance growth, there could nevertheless be substantial but transient short-time energy amplification. The implication was that this energy growth could amplify a small disturbance into one which could trigger the transition to turbulence seen in experiments through nonlinear processes, although the analysis was strictly only linear (substantially amplified infinitesimal disturbances are still only infinitesimal). Interestingly, this new formulation revolved around considering the evolution of a mixture of normal modes rather than just one in isolation and revealed how the non-orthogonality of these modes with each other (present when the linearised operator is non-normal) can lead to short-time energy growth. The initial and final disturbances of the energy growth episode have very different spatial structures - hence the term ‘non-modal’ analysis - whereas in linear stability, or ‘modal’ analysis, the normal modes maintain their spatial structure as they evolve.

Slightly after this nonmodal approach had completed the linear perspective of stability in the early 1990s, an alternative fully nonlinear dynamical systems approach started to emerge. This was sparked by the discovery of new finite amplitude solutions disconnected from the reference state in shear flows (see the reviews Kerswell 2005, Eckhardt et al. 2007, Kawahara et al. 2012) and was made feasible by the increasing availability of computational power. In this approach, the flow is viewed as a (huge) dynamical system in which the flow state evolves along a trajectory in a phase space populated by various invariant sets (exact solutions) and their stable and unstable manifolds. In the case of a linearly-stable reference state, transition or ‘nonlinear instability’ occurs when a finite disturbance to the system puts the flow state beyond the basin of attraction of the reference state in phase space. The dynamical systems approach to transition focuses on fully nonlinear structures like basin boundaries and what happens beyond them whereas nonmodal analysis describes how infinitesimal disturbances can grow temporarily in the immediate neighbourhood of

---

**Non-Normal:** An operator/matrix  $L$  is non-normal if it does not commute with its adjoint/transpose  $L^\dagger$ , i.e.  $LL^\dagger \neq L^\dagger L$ .

---

the reference state deep within the basin of attraction.

Recently a theoretical technique, which is the nonlinear extension of nonmodal analysis, has been developed to bridge this gap in perspective and disturbance amplitude. Conceptually, the addition of nonlinearity to (linear) nonmodal analysis is a simple step and as a result has been formulated independently in (at least) three different parts of the scientific literature over the last 15 years (in transitional flows by Pringle & Kerswell 2010, Cherubini et al. 2010 and Monokrousos et al. 2011 - see §4.1; in oceanography by Mu et al. 2004 - see §5.1; and in thermoacoustics by Juniper 2011a - see §5.2). Mathematically, however, nonlinearity changes everything. What was a convex optimization problem to maximise energy growth with a unique optimiser now becomes a fully nonlinear, non-convex optimization problem where much less is known about the possibly multiple solutions (local as well as global maxima) or how to find them. However, the key recent advance has been the realisation that such problems are now solvable for the 3D Navier-Stokes equation discretised by a large number ( $O(10^5-10^6)$ ) of degrees of freedom (Pringle & Kerswell 2010, Cherubini et al. 2010, Monokrousos et al. 2011) by using a direct-adjoint looping approach on a desktop computer. That this is a step up in computational complexity, however, is reflected in the fact that the first nonlinear energy growth optimals incorporating the full 3D Navier-Stokes equations were computed (Pringle & Kerswell 2010, Cherubini et al. 2010) fully 18 years after the first 3D linear energy growth optimal (Butler & Farrell 1992).

### Nonlinear Stability

The nonlinear stability of a reference state is usually couched in terms of how an energy norm  $E(t)$  (e.g. the kinetic energy) of any disturbance to the reference state evolves in time. If  $\lim_{t \rightarrow \infty} E(t)/E(0) = 0$  for all  $E(0) \leq \delta$ , where  $\delta$  is finite, then the reference state is nonlinearly stable and  $\delta$  measures how stable.

In its simplest form, nonlinear nonmodal analysis seeks to identify the disturbance from among all disturbances of a given energy  $E(0)$  which optimises the energy growth,  $G(E(0), T) := E(T)/E(0)$ , some time  $T$  later. While the result of (linear) nonmodal analysis is recovered when  $E(0) \rightarrow 0$ , increasing  $E(0)$  explores ever more distant parts of the basin of attraction away from the reference state. If  $E(0)$  is increased enough, the set of competing disturbances includes initial conditions outside the basin of attraction which is reflected in a step change in the optimal energy gain found. Determining the critical starting energy value when this occurs identifies the finite-amplitude disturbance which first breaches the basin boundary of the reference state. In this way nonlinear nonmodal analysis coupled with a search over the initial energy  $E(0)$  represents a nonlinear stability analysis - called ‘nonlinear nonmodal stability analysis’ here - since the most ‘dangerous’ disturbance which can cause the system to evolve to another state is found together with a measure of how nonlinearly stable the reference state is in the form of the minimal energy needed to initiate this event. The purpose of this review is to describe the results found so far using this nonlinear nonmodal stability analysis and to highlight the huge potential for new applications. An earlier progress report (Kerswell et al. 2014) emphasized the generality of this approach as a fully nonlinear optimization technique for studying nonlinear systems whereas here the focus is on its use to probe nonlinear stability in fluid mechanics and the fact that it is a natural extension of (linear) nonmodal stability analysis in hydrodynamic stability, as

reviewed a decade ago by Schmid (2007).

## 2. Overview

The plan of this review is to first explain in §3 the procedure for performing nonlinear nonmodal analysis which, in its simplest form, is the procedure of finding the optimal energy growth over all disturbances of a given starting energy and time horizon constrained by the 3D Navier-Stokes equation for an incompressible fluid. This is the fundamental, fully-nonlinear optimization problem which underpins everything that follows. The objective functional to be optimised needn't be the energy, nor must the initial amplitude constraint also be the energy, but these simple choices are the most logical historically (nonmodal analysis focusses on this), natural mathematically and illustrate the phenomenology most clearly. A series of subsequent sections then outline how the results of this optimization procedure - the optimal disturbance at one choice of the initial energy and target time - can then be utilised in different ways to study the nonlinear stability of a linearly-stable reference state. It is this two-tier process of nonlinear nonmodal analysis coupled to, say, a subsequent search over the initial energy which constitutes the nonlinear nonmodal stability theory titling this article.

The primary application so far has been in bistable systems where the disturbance of smallest energy to trigger transition from one state (typically a steady laminar flow) to the other (a turbulent state) is sought: see §4.1. Section 4.2 discusses the use of nonlinear nonmodal analysis to identify different types of transition scenario, where, for example the flow undergoes a 'bursting' (large energy event) before settling down to the (lower energy) turbulent state, or rapid transition is required (turbulence is reached after a given time rather than asymptotically long times). §4.3 then describes preliminary work directed at identifying nearby unstable solutions to the reference state which is the only attractor in the system. This scenario is now realised to be quite a common situation in low Reynolds number shear flows and being able to identify when new alternative solutions appear in phase space as the Reynolds number increases is of key importance in anticipating the emergence of a chaotic repeller. §4.4 discusses the issue of how the analysis can be modified to probe the nonlinear stability of a time-dependent reference state. Here little has been done but there is great potential to make progress. Finally, other applications are briefly discussed which use the same looping procedure to solve related optimization problems. These are mentioned to give further evidence that the whole approach of solving highly nonlinear constrained optimization problems using a looping approach is now both feasible and a valuable theoretical approach. The article closes with a summary and discussion of future directions.

## 3. Nonlinear Nonmodal Analysis

### 3.1. Formulation

The procedure for nonlinearising nonmodal analysis is described here using the example of an incompressible fluid in steady unidirectional flow  $\mathbf{U}(\mathbf{x})$  driven by a combination of applied pressure gradient and boundary conditions (the particular situation of pipe flow is discussed in Kerswell et al. 2014). For clarity, we discuss the formulation using the simplest choices of the energy at a time  $T$  later as the objective functional and the energy norm to measure the size of the initial perturbation. We assume that there exists a simple

basic state  $(\mathbf{U}, P)$  directly driven by the inhomogeneities of the problem and work with the disturbance fields  $(\mathbf{u}, p)$  away from this basic state,

$$\mathbf{u} := \mathbf{u}_{\text{tot}} - \mathbf{U}, \quad p = p_{\text{tot}} - P, \quad (1)$$

(where  $(\mathbf{u}_{\text{tot}}, p_{\text{tot}})$  are the full fields) which satisfy the unforced Navier Stokes equation

$$\frac{\partial \mathbf{u}}{\partial t} + (\mathbf{U} \cdot \nabla) \mathbf{u} + (\mathbf{u} \cdot \nabla) \mathbf{U} + (\mathbf{u} \cdot \nabla) \mathbf{u} + \nabla p - \frac{1}{Re} \nabla^2 \mathbf{u} = \mathbf{0}, \quad (2)$$

are incompressible

$$\nabla \cdot \mathbf{u} = 0 \quad (3)$$

and obey homogeneous boundary conditions (by default non-slip on solid surfaces and periodicity in any unbounded direction). Then to extremise the objective functional, the Lagrangian

$$\begin{aligned} \mathcal{L} = \mathcal{L}(\mathbf{u}, p, \lambda, \boldsymbol{\nu}, \pi; T, E_0) &:= \left\langle \frac{1}{2} |\mathbf{u}(\mathbf{x}, T)|^2 \right\rangle + \lambda \left\{ \left\langle \frac{1}{2} |\mathbf{u}(\mathbf{x}, 0)|^2 \right\rangle - E_0 \right\} \\ &+ \int_0^T \left\langle \boldsymbol{\nu}(\mathbf{x}, t) \cdot \left\{ \frac{\partial \mathbf{u}}{\partial t} + (\mathbf{U} \cdot \nabla) \mathbf{u} + (\mathbf{u} \cdot \nabla) \mathbf{U} + (\mathbf{u} \cdot \nabla) \mathbf{u} \right. \right. \\ &\quad \left. \left. + \nabla p - \frac{1}{Re} \nabla^2 \mathbf{u} \right\} \right\rangle dt + \int_0^T \langle \pi(\mathbf{x}, t) \nabla \cdot \mathbf{u} \rangle dt \end{aligned} \quad (4)$$

is considered where

$$\langle \dots \rangle := \iiint \dots dV \quad (5)$$

and  $\lambda$ ,  $\boldsymbol{\nu}$  and  $\pi$  are Lagrange multipliers imposing the constraints that the amplitude of the initial disturbance is fixed, that the Navier-Stokes equation holds over  $t \in [0, T]$  and that the flow is incompressible. Their corresponding Euler-Lagrange equations are

$$\left\langle \frac{1}{2} |\mathbf{u}(\mathbf{x}, 0)|^2 \right\rangle = E_0 \quad (6)$$

together with (2) and (3) respectively. The linearised problem is recovered in the limit of  $E_0 \rightarrow 0$  whereupon the nonlinear term  $\mathbf{u} \cdot \nabla \mathbf{u}$  becomes vanishingly small relative to the other (linear) terms. On dropping this nonlinear term, the amplitude of the disturbance is then arbitrary for the purposes of the optimization calculation and it is convenient to reset  $E_0$  from vanishingly small to 1. In this case the maximum of  $\mathcal{L}$  is then precisely the maximum *gain* in energy over the period  $[0, T]$ .

The variation of  $\mathcal{L}$  with respect to the pressure  $p$  is

$$\int_0^T \left\langle \frac{\delta \mathcal{L}}{\delta p} \delta p \right\rangle dt = \int_0^T \langle (\boldsymbol{\nu} \cdot \nabla) \delta p \rangle dt = \int_0^T \langle \nabla \cdot (\boldsymbol{\nu} \delta p) \rangle dt - \int_0^T \langle \delta p (\nabla \cdot \boldsymbol{\nu}) \rangle dt \quad (7)$$

which vanishes if  $\boldsymbol{\nu}$  is incompressible and satisfies natural boundary conditions that mirror those for  $\mathbf{u}$  (note  $\delta p$  is periodic in any homogeneous directions to ensure any imposed pressure drop across the system is constant). The variation in  $\mathcal{L}$  due to  $\mathbf{u}$  (with  $\delta \mathbf{u}$  vanishing

on boundaries and periodic in homogeneous direction) is

$$\begin{aligned} \delta\mathcal{L} = & \int_0^T \left\langle \frac{\delta\mathcal{L}}{\delta\mathbf{u}} \cdot \delta\mathbf{u} \right\rangle = \langle \mathbf{u}(\mathbf{x}, T) \cdot \delta\mathbf{u}(\mathbf{x}, T) \rangle + \lambda \langle \mathbf{u}(\mathbf{x}, 0) \cdot \delta\mathbf{u}(\mathbf{x}, 0) \rangle \\ & + \int_0^T \left\langle \boldsymbol{\nu} \cdot \left\{ \frac{\partial\delta\mathbf{u}}{\partial t} + (\mathbf{U} \cdot \nabla)\delta\mathbf{u} + (\delta\mathbf{u} \cdot \nabla)\mathbf{U} + \mathbf{u} \cdot \nabla\delta\mathbf{u} + \delta\mathbf{u} \cdot \nabla\mathbf{u} \right. \right. \\ & \left. \left. - \frac{1}{Re}\nabla^2\delta\mathbf{u} \right\} \right\rangle dt + \int_0^T \langle \pi \nabla \cdot \delta\mathbf{u} \rangle dt. \quad (8) \end{aligned}$$

Integration by parts both in time and space allows this to be re-expressed as

$$\begin{aligned} \int_0^T \left\langle \frac{\delta\mathcal{L}}{\delta\mathbf{u}} \cdot \delta\mathbf{u} \right\rangle = & \langle \delta\mathbf{u}(\mathbf{x}, T) \cdot \{\mathbf{u}(\mathbf{x}, T) + \boldsymbol{\nu}(\mathbf{x}, T)\} \rangle + \langle \delta\mathbf{u}(\mathbf{x}, 0) \cdot \{\lambda\mathbf{u}(\mathbf{x}, 0) - \boldsymbol{\nu}(\mathbf{x}, 0)\} \rangle \\ & + \int_0^T \left\langle \delta\mathbf{u} \cdot \left\{ -\frac{\partial\boldsymbol{\nu}}{\partial t} - ([\mathbf{U} + \mathbf{u}] \cdot \nabla)\boldsymbol{\nu} + \boldsymbol{\nu} \cdot (\nabla[\mathbf{U} + \mathbf{u}])^T \right. \right. \\ & \left. \left. - \nabla\pi - \frac{1}{Re}\nabla^2\boldsymbol{\nu} \right\} \right\rangle dt \quad (9) \end{aligned}$$

where  $[\boldsymbol{\nu} \cdot (\nabla[\mathbf{U} + \mathbf{u}])^T]_i = \nu_j \partial_i (U_j + u_j)$ . A little care is needed in treating the incompressibility constraint as the surface term generated

$$\langle \pi \nabla \cdot \delta\mathbf{u} \rangle = \langle \nabla \cdot \pi \delta\mathbf{u} \rangle - \langle \delta\mathbf{u} \cdot \nabla \pi \rangle \quad (10)$$

only drops if  $\pi$  is periodic in the applied pressure gradient direction as  $\langle \delta\mathbf{u} \cdot \nabla p_{tot} / |\nabla p_{tot}| \rangle \neq 0$  (a change in the mass flux is permitted for constant pressure-drop driven flow). Imposing constant mass flux, as is usual in pipe flow (see Pringle & Kerswell 2010, Pringle et al. 2012), releases  $\pi$  from this restriction but then, via (7) forces  $\boldsymbol{\nu}$  to also have zero flux.

For the first variation of  $\mathcal{L}$ ,  $\delta\mathcal{L}$  in (8), to vanish for all allowed  $\delta\mathbf{u}(\mathbf{x}, T)$ ,  $\delta\mathbf{u}(\mathbf{x}, 0)$  and  $\delta\mathbf{u}(\mathbf{x}, t)$  with  $t \in (0, T)$  requires

$$\frac{\delta\mathcal{L}}{\delta\mathbf{u}(\mathbf{x}, T)} = \mathbf{0} \quad \Rightarrow \quad \mathbf{u}(\mathbf{x}, T) + \boldsymbol{\nu}(\mathbf{x}, T) = \mathbf{0}, \quad (11)$$

$$\frac{\delta\mathcal{L}}{\delta\mathbf{u}(\mathbf{x}, 0)} = \mathbf{0} \quad \Rightarrow \quad \lambda\mathbf{u}(\mathbf{x}, 0) - \boldsymbol{\nu}(\mathbf{x}, 0) = \mathbf{0}, \quad (12)$$

$$\frac{\delta\mathcal{L}}{\delta\mathbf{u}(\mathbf{x}, t)} = \mathbf{0} \quad \Rightarrow \quad \frac{\partial\boldsymbol{\nu}}{\partial t} + (\mathbf{U} + \mathbf{u}) \cdot \nabla\boldsymbol{\nu} - \boldsymbol{\nu} \cdot (\nabla[\mathbf{U} + \mathbf{u}])^T + \nabla\pi + \frac{1}{Re}\nabla^2\boldsymbol{\nu} = \mathbf{0}. \quad (13)$$

This last equation is the dual (or adjoint) Navier-Stokes equation for evolving  $\boldsymbol{\nu}$  backwards in time because of the negative diffusion term and is linear in  $\boldsymbol{\nu}$ . This dual equation has the same means of driving - constant pressure drop - as the physical problem, a situation also true for the constant mass-flux situation (e.g. see Pringle & Kerswell 2010, Pringle et al. 2012 for the pipe flow problem).

### 3.2. Solution Procedure

The approach for tackling this optimization problem - ‘nonlinear direct-adjoint looping’ - is iterative as in the linear situation (Luchini & Bottaro 1998, Anderson et al. 1999, Luchini 2000, Corbett & Bottaro 2000, Guégan et al 2006, see also the review Luchini & Bottaro 2014), the nonlinear calculations of Zuccher et al. (2004, 2006) using the (parabolic)

boundary layer equations and more generally (Gunzburger 2000). The procedure is started by choosing an initial condition  $\mathbf{u}^{(0)}(\mathbf{x}, 0)$  such that

$$\left\langle \frac{1}{2} |\mathbf{u}^{(0)}(\mathbf{x}, 0)|^2 \right\rangle = E_0. \quad (14)$$

This can be any flow field which satisfies the boundary conditions but in practice it is best to ensure that it is also incompressible: a renormalised turbulent state seems to work well even computed at a different *Re*. The (better) next iterate  $\mathbf{u}^{(n+1)}(\mathbf{x}, 0)$  is then constructed from  $\mathbf{u}^{(n)}(\mathbf{x}, 0)$  via the following 4 steps which are repeated until some convergence criterion is reached (Kerswell et al. 2014).

**Step 1.** Time integrate the Navier-Stokes equation (2) forward from  $t = 0$  to  $t = T$  imposing incompressibility (3) with the initial condition  $\mathbf{u}^{(n)}(\mathbf{x}, 0)$  to find  $\mathbf{u}^{(n)}(\mathbf{x}, T)$ .

**Step 2.** Calculate  $\boldsymbol{\nu}^{(n)}(\mathbf{x}, T)$  using (11) which is then used as the initial condition for the dual Navier-Stokes equation (13).

**Step 3.** Backwards in time integrate the dual Navier-Stokes equation (13) from  $t = T$  to  $t = 0$  with the ‘initial’ condition  $\boldsymbol{\nu}^{(n)}(\mathbf{x}, T)$  to find  $\boldsymbol{\nu}^{(n)}(\mathbf{x}, 0)$ .

**Step 4.** Use the fact that

$$\frac{\delta \mathcal{L}}{\delta \mathbf{u}(\mathbf{x}, 0)} = \lambda \mathbf{u}(\mathbf{x}, 0) - \boldsymbol{\nu}(\mathbf{x}, 0) \quad (15)$$

is now computable to move  $\mathbf{u}(\mathbf{x}, 0)$  towards a maximum of  $\mathcal{L}$ . There are a multitude of possible approaches that can be used here. One approach (Pringle & Kerswell 2010, Pringle et al. 2012, Rabin et al. 2012) is to simply move  $\mathbf{u}^{(n)}(\mathbf{x}, 0)$  in the direction of maximum ascent of  $\mathcal{L}$ , i.e. a correction to  $\mathbf{u}^{(n)}$  is calculated as follows:

$$\mathbf{u}^{(n+1)} = \mathbf{u}^{(n)} + \epsilon \left[ \frac{\delta \mathcal{L}}{\delta \mathbf{u}(\mathbf{x}, 0)} \right]^{(n)} = \mathbf{u}^{(n)} + \epsilon \left( \lambda \mathbf{u}^{(n)}(\mathbf{x}, 0) - \boldsymbol{\nu}^{(n)}(\mathbf{x}, 0) \right), \quad (16)$$

with  $\lambda$  chosen to ensure that

$$E_0 = \left\langle \frac{1}{2} |\mathbf{u}^{(n+1)}(\mathbf{x}, 0)|^2 \right\rangle = \left\langle \frac{1}{2} |(1 + \epsilon \lambda) \mathbf{u}^{(n)}(\mathbf{x}, 0) - \epsilon \boldsymbol{\nu}^{(n)}(\mathbf{x}, 0)|^2 \right\rangle. \quad (17)$$

Here  $\epsilon$  is a parameter which can be adjusted as the iteration proceeds to improve convergence (e.g. Pringle et al. 2012, Rabin et al. 2012). (The same procedure can be used to solve the linearised problem but with step 4 replaced by simply setting  $\mathbf{u}(\mathbf{x}, 0)$  equal to  $\boldsymbol{\nu}(\mathbf{x}, 0)$  or a rescaled version of it: this is known as the power method - e.g. see Corbett & Bottaro 2000.) Other strategies have been adopted - e.g. a relaxation approach (Monokrousos et al. 2011, Duguet et al. 2013), a conjugate gradient method (Cherubini et al. 2010, 2011, 2012, Cherubini & De Palma 2013, Juniper 2011a) and a gradient rotation method (Farano et al. 2016, 2017). Evidence for which approach is best is anecdotal and probably varies with the situation. No one method stands out when compared in the pipe flow problem using a convergence criterion based on the residual - see §3.2.1 (Pringle, private communication) whereas the gradient rotation method has been found to converge in about 10 times less iterations than a standard steepest ascent approach in 2D Poiseuille flow using an incremental change criterion - again see §3.2.1 (Cherubini, private communication).

**3.2.1. Convergence .** So far two different convergence criteria have been adopted: one based on the  $L^2$  norm of the residual  $\langle(\delta\mathcal{L}/\delta\mathbf{u}(\mathbf{x},0))^2\rangle$  (Pringle & Kerswell 2010, Pringle et al. 2012, Rabin et al. 2012) and the other on the incremental change in  $\mathcal{L}$  between iterations (Cherubini et al. 2010, 2011, 2012, Cherubini & De Palma 2013). The danger with the latter is that it can become small because of the size of the step taken in  $\mathbf{u}(\mathbf{x},0)$  rather than because  $\delta\mathcal{L}/\delta\mathbf{u}(\mathbf{x},0)$  is vanishing. The former also has problems with the residual sometimes failing to keep decreasing even when there is no apparent further increase in the objective functional (e.g. Figure 9 in Pringle et al. 2012, Figure 9(b) in Rabin et al. 2012, and the top (left) plot in **Figure 5**). This ‘stalling’ of the iterative procedure despite an apparently good optimal emerging is not currently understood.

**3.2.2. Checkpointing.** One key new feature of the looping procedure when the full Navier-Stokes equation is incorporated as a constraint is that the dual Navier-Stokes equation now depends on  $\mathbf{u}$ . To avoid storing  $\mathbf{u}$  in totality (which is impractical for all but the smallest calculations), ‘checkpointing’ (Berggren 1998, Hinze et al. 2006) is used in which  $\mathbf{u}$  is recalculated piecemeal during the backward integration stage. This requires storing  $\mathbf{u}$  at regular intermediate points, e.g.  $t = T_i := iT/n$  for  $i = 1, \dots, n - 1$ , during the forward integration stage. Then, to integrate the adjoint equation backward over the time interval  $[T_i, T_{i+1}]$ ,  $\mathbf{u}$  is regenerated starting from the stored value at  $t = T_i$  by integrating the Navier-Stokes equations forward to  $T_{i+1}$  again. The number of intermediate points is chosen such that the storage requirement for each subinterval is manageable (preferably in memory rather than stored on disk). The extra overhead of this technique is to redo the forward integration for every backward integration, approximately a 50% increase in cpu time, assuming forward and backward integrations take essentially the same time and ignoring any occasional state reads from disk.

**3.2.3. Robustness.** The hope is that the looping approach uncovers the global optimizer but, since the optimization problem is nonlinear and non-convex, there is unlikely ever be a way to confirm this. A practical way to get some reassurance is to initiate the optimization procedure with a suite of very different initial conditions every so often to see if the same global optimal emerges (e.g. see Figures 14 and 15 of Pringle et al. 2012).

### 3.3. Results

The above has discussed the procedure to (hopefully) find a global optimal initial condition  $\mathbf{u}_{\mathbf{NL}}^{\text{opt}}(\mathbf{x})$  of a given energy amplitude  $E_0$  which maximises the objective functional using the specific example of energy growth after time  $T$ . Here we discuss what results emerge as a function of  $T$  and  $E_0$  since formally  $\mathbf{u}_{\mathbf{NL}}^{\text{opt}} = \mathbf{u}_{\mathbf{NL}}^{\text{opt}}(\mathbf{x}; Re, E_0, T)$  (suppressing any dependence on flow geometry) at a given  $Re$ . Clearly,

$$\lim_{E_0 \rightarrow 0} \mathbf{u}_{\mathbf{NL}}^{\text{opt}}(\mathbf{x}; Re, E_0, T) = \mathbf{u}_{\mathbf{L}}^{\text{opt}}(\mathbf{x}, Re, T), \quad (18)$$

where  $\mathbf{u}_{\mathbf{L}}^{\text{opt}}(\mathbf{x}; Re, T)$  is the optimal which extremises the objective functional constrained by the *linearised* Navier-Stokes equations (referred to as the LOP - ‘linear optimal perturbation’; Pringle et al. 2012, 2015, Rabin et al. 2012). There has to be, of course, a finite neighbourhood  $0 \leq E_0 \leq E_{NL}(Re, T)$  in which  $\mathbf{u}_{\mathbf{NL}}^{\text{opt}}$  gradually moves away from  $\mathbf{u}_{\mathbf{L}}^{\text{opt}}$  as  $E_0$  increases from 0 due to the effects of nonlinearity. This nonlinearly-adjusted linear optimal is sometimes referred to as the ‘quasi-linear optimal perturbation’ or QLOP - e.g.

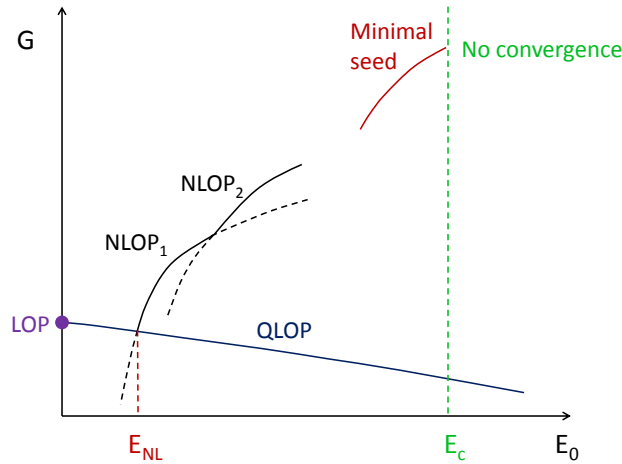


**Figure 1**

(a) A sketch of how the maximum energy gain  $G = E(T)/E(0)$  varies with  $E(0) = E_0$ . At  $E_0 = 0$ , the linear optimal (LOP) is found, for small  $E_0 < E_{NL}$  the optimal is a nonlinearly-adjusted version of the LOP called the quasi-linear optimal perturbation (QLOP). At  $E_{NL}$  a qualitatively different optimal emerges - the nonlinear optimal perturbation (NLOP<sub>1</sub>) which is typically localised. Further NLOPs can emerge as  $E_0$  increases further until the looping algorithm fails to converge at  $E_c$  if the target state is turbulent. The optimal NLOP converged in the limit  $E_0 \rightarrow E_c^-$  is the minimal seed for transition to the new target state.

Rabin et al. (2012). Beyond  $E_{NL}$  (the ‘nonlinearity threshold’ in Cherubini et al. 2011, 2012), however, a completely different global optimal emerges - called the nonlinear optimal perturbation or NLOP. This was first observed in pipe flow (Pringle & Kerswell 2010 with  $T$  set as that which produces the largest growth in the linear problem) where the change is particularly stark because  $\mathbf{u}_L^{\text{opt}}$  and hence also the QLOP are invariant along the pipe (Schmid & Henningson 1994) whereas the new nonlinear optimal that emerges beyond  $E_{NL}$  is fully 3-dimensional (Pringle & Kerswell 2010). The most striking difference, however, is that the new  $\mathbf{u}_{NL}^{\text{opt}}$  is localised in the flow domain - rolls and streaks of comparable amplitude localised to one side of the short pipe studied - whereas  $\mathbf{u}_L^{\text{opt}}$  is global consisting of a pair of pipe-filling counterrotating streamwise rolls ( see Figure 2 of Pringle & Kerswell 2010 and Pringle et al. 2015 which demonstrate full localisation of the NLOP in a long pipe domain). This spatial localisation is a generic feature which allows the perturbation to have a larger peak amplitude to exploit the nonlinear mechanisms present but only over a limited volume to cheat the global energy constraint. In contrast, by linearity,  $\mathbf{u}_L^{\text{opt}}$  is a global Fourier mode in every homogeneous direction, typically of long wavelength to minimise viscous decay and so global in the boundary-normal direction as well.

As  $E_0$  is increased beyond  $E_{NL}$ , further, structurally different NLOPs can emerge as global optimisers (e.g. in plane Couette flow: Rabin et al. 2012, Cherubini & De Palma 2013) or not (e.g. in pipe flow: Pringle & Kerswell 2010, Pringle et al. 2012, 2015) before, assuming turbulence coexists with the base flow, the algorithm eventually fails to converge beyond a value  $E_0 = E_c(T; Re)$  (Pringle et al. 2012): see **Figure 1**. At this point,

---

**LOP:** The optimal found using linear nonmodal analysis

**QLOP:** The nonlinearly adjusted version of the LOP.

**NLOP:** An optimal which bears no relation to the LOP or QLOP and critically relies on the nonlinearity of the governing equations to exist.

---

the looping scheme has stumbled across an initial condition in the basin of attraction of the turbulence which can reach the turbulent state by the target time. As a result, the looping procedure becomes ill-conditioned due to the extreme sensitivity of the final state energy to changes in the initial condition (Pringle et al. 2012). Reducing  $T$  allows NLOPs to be converged at higher initial energies (Cherubini et al 2010, 2011, Cherubini & De Palma 2013, Farano et al. 2015) whereas increasing  $T$  reduces  $E_c(T; Re)$ . This implies the existence of a minimal finite (since the base flow is linearly stable) value  $E_c(\infty; Re)$  which represents the infimum on the disturbance energy which can trigger transition or, equivalently, equals the minimum energy of any state on the laminar-turbulent boundary or edge. States arbitrarily close to this minimal energy state - called the ‘minimal seed’ (Pringle et al. 2012) - and ‘above’ the edge (so outside the basin of attraction of the laminar state) trigger turbulence. The closer they are to the minimal seed, the longer they take to reach the turbulent state. Finding the form of the minimal seed is therefore central to understanding transition in threshold conditions, that is, where transition is just triggered. The evolution of the minimal seed itself is within the laminar-turbulent boundary or edge, which is an invariant manifold, and is ultimately attracted to a relative attractor embedded with it. This can be unique and simple (e.g. the equilibrium in Schneider et al. 2008) but more generally is non-unique (§3.6 of Duguet et al. 2008) and chaotic (e.g. Schneider et al. 2007, Mellibovsky et al. 2009). Either way, the minimal seed itself does not lead to turbulence but there are states arbitrarily close to it which do. Identifying it is the first application of the basic optimization approach just discussed.

---

**Edge:** The edge is a hypersurface in phase space which separates flow states which evolve in qualitatively different ways.

---

## 4. Nonlinear Nonmodal Stability Analysis

### 4.1. Switching Basins of Attraction: Minimal Seeds for Transition

The approach to calculating the minimal seed assumes that as the disturbance energy hypersurface expands (i.e.  $E_0$  increases), it first touches the laminar-turbulent boundary or edge at precisely the energy  $E_0 = E_c(T; Re)$  (e.g. see the simple 2 ODE model of §2.1 in Kerswell et al. 2014). The common state on the two manifolds is then the minimal seed as it has the lowest energy state on the edge. For  $E_0 > E_c$ , so that now the edge punctures the energy hypersurface, there exist initial conditions for the optimization procedure which are in the basin of attraction of the turbulent state (or more generally are ‘above’ the edge if the turbulence is instead a chaotic saddle). These can then achieve values of the objective functional larger than any possible in the laminar basin of attraction (by design) and so the optimization will track these. If the subsequent evolutions reach the turbulent state, the looping algorithm will then fail to converge due to extreme sensitivity to the initial conditions unless the objective functional has been specifically designed to average over the final turbulent state in some way (Monokrousos et al. 2011). The procedure is then to slowly increase  $E_0$  from a value where the algorithm converges until it no longer does due to the existence of turbulent end states created by the looping iterates. The optimal of the last successful convergence at  $E_0 \lesssim E_c(T; Re)$  is an approximation to the minimal seed providing  $T$  is large enough (Pringle et al. 2012). A complementary approach is to start with  $E_0 \gtrsim E_c$  where ‘turbulent seeds’ - initial conditions which lead to turbulence by  $T$  - can be identified and then gradually reducing  $E_0$  (initiating with the previously identified turbulent seeds at slightly higher  $E_0$ ) until no turbulent seeds can be found (Monokrousos

et al. 2011, Rabin et al. 2012, 2014). This latter approach can be quite efficient if the starting  $E_0$  is sufficiently close to  $E_c$  as then the set of turbulent seeds will shrink down smoothly to the minimal seed as  $E_0 \rightarrow E_c^+$ , although there is always the danger of settling on a local rather than global energy minimum of the edge.

Pringle et al. (2012) argue for why energy growth after time  $T$  might be the most natural objective functional for this procedure, but actually any objective functional which takes on heightened values in the basin of attraction of the turbulent state will do (e.g. total dissipation over the trajectory - Monokrousos et al. 2011, Duguet et al 2013 and Eaves & Caulfield 2015). The key point is that the optimization procedure should seek out any initial condition on the energy hypersurface which is in the turbulent basin of attraction if such states maximise the objective functional. Rabin et al. (2012) confirmed that the same minimal seed emerged in plane Couette flow by using energy growth after time  $T$  as when the total dissipation was used (Monokrousos et al. 2011). Practically,  $T$  has to be chosen large enough to find the (globally) minimal seed and  $E_c(T; Re)$  rather than just local minima. However, evidence gathered so far using a variety of different  $T$  indicates that this is not such a problem. For example, the NLOP first found in Pringle & Kerswell (2010) (see their Figure 2) using a pipe only  $\pi/2$  diameters long at  $Re = 1750$  and  $T = 21 D/U$  (where  $D$  is the pipe diameter and  $U$  is the mean flow along the pipe) is recognisably the same structure (albeit with no streamwise localisation and an extra symmetry: see Figure 8 of Pringle et al. 2015) as that found at  $Re = 2400$  in a pipe  $5D$  long using  $T = 75 D/U$  (see §5 of Pringle et al. 2012) and in a pipe  $50D$  long using  $T = 29.35 D/U$ . In fact, the latter study was able to reduce  $T$  down to  $\approx 16 D/U$  before finding any significant structural change in the NLOP. There is also further indirect evidence for this robustness to the choice  $T$  in that similar optimals are reported across a variety of flows: in plane Couette flow (Cherubini & De Palma 2013, 2014a); the Blasius boundary layer (Cherubini et al. 2010, 2011, 2012); the asymptotic suction boundary layer (Cherubini et al. 2015) and plane Poiseuille flow (Farano et al. 2015, 2016). If  $T$  is too small, transients can obscure the situation (Rabin et al. 2012) or new optimals become preferred (Pringle et al. 2015, Farano 2015). Another potential problem is studying a flow where the turbulent state is not separated from the laminar-turbulent boundary or edge as far as the objective functional is concerned. This is a well-known issue with the technique of edge-tracking (Schneider & Eckhardt 2009) and experience gained there indicates that provided the flow is not too tightly constrained (e.g. the computational box is not too small) or too close to the first appearance of the turbulent state ( $Re$  too low), the required separation exists.

**4.1.1. Evolution.** Once the minimal seed has been found, the evolution of a nearby turbulent seed can be studied to uncover the optimal way (initiated by a disturbance of least energy) to trigger transition. The fairly robust picture which emerges is that the minimal seed is always spatially localised in all directions to allow much larger velocity amplitudes to be accommodated than would be possible globally given the initial amplitude constraint (for example see **Figure 2**). The minimal seed is also characterised by an initial flow pattern which opposes the underlying mean shear so as to immediately benefit from the Orr mechanism (Orr 1907). In this, the mean shear rotates the disturbance field around to align with the mean flow direction creating some initial disturbance energy growth over a fast time scale. Concurrently, the minimal seed also delocalises or ‘smears out’ due to the mean shear before an ‘oblique wave phase’ of energy growth occurs over intermediate time scales. This passes its energy into streamwise rolls which initiate a third growth process



**Figure 2**

The evolution of an initial condition close to but ‘below’ the minimal seed in a pipe  $25D$  (diameters) long with  $t = 0, 0.25, 0.5, 1, 2.5, 5, 10, 20$  and  $T_{opt} = 29.35 D/U$  (going downwards: flow is from left to right) where  $U$  is the bulk speed along the pipe and  $Re := UD/\nu = 2400$  (see figures 1 and 3 from Pringle et al. (2015) for alternative representations of the evolution) The initially localised disturbance grows locally in amplitude and spatial extent evolving into an almost axially-invariant streak structure.

known as ‘lift up’ which operates over a comparatively slow (viscous) time scale (Pringle et al. 2012, Duguet et al. 2013) to produce a predominately 2-dimensional streak field (e.g. see the last 2 snapshots in **Figure 2**). For an initial condition just below the edge, this streak field is linearly stable and the flow will ultimately decay. For an initial condition on the edge, the streak field will then evolve into the (attracting) edge state whereas for an initial condition just above the edge, the streak field is unstable, starts to bend and breaks down to small scales signalling the turbulence state (e.g. Figure 12 of Pringle et al. 2012 and Duguet et al. 2013).

What is intriguing and also reassuring about this evolution is the fact that the finite-amplitudeness of the minimal seed is able to symbiotically couple together - via the nonlinearity of the Navier-Stokes equations - three well-known linear growth mechanisms which are staggered in time scale but uncoupled in the linearised Navier-Stokes equations. The Orr mechanism is essentially a 2D spanwise-invariant process, while the oblique wave growth is inherently 3D and the lift-up mechanism is optimised by 2D streamwise-invariant flows. The minimal seed is able to take advantage of all 3 processes in turn by ensuring that the energy growth of the preceding process is available to seed the next: see Appendix B of Kerswell et al. (2014) for a simple example of this. The fact that retaining the nonlinearity can then link these processes up is reassuring that the truly optimal (global) minimal seed has been revealed by this procedure.

Essentially the same picture emerges from the Blasius boundary layer calculations of Cherubini et al. (2011, 2012) although they work with short  $T$  and analyse a NLOP computed some way ‘over’ the laminar-turbulent boundary rather than the minimal seed. Although this NLOP seems to have the same localised structure - vortices inclined to the streamwise direction positioned on the flanks of a region of intense streamwise velocity, the various dynamical processes are not so well separated in time to the extent that the formation of streaks and their subsequent instability are obscured by other instabilities. Interestingly, they identify coherent structures reminiscent from DNS such as  $\Lambda$  vortices and hairpin vortices in the evolution (e.g. see Figure 22 of Cherubini et al. 2011). Hairpin vortices are also found to be generated by optimals computed in plane Poiseuille flow using a very short  $T$  on the timescale of the Orr mechanism (Farano et al. 2015).

Once the minimal seed has been identified, its critical energy  $E_c$  can then be tracked as a function of  $Re$ . This has been attempted in plane Couette flow at least up to  $Re = 3000$  which suggests a scaling law  $E_c = O(Re^{-2.7})$  for the transition threshold (Duguet et al. 2013). This is significantly smaller than previous estimates of  $E_c = O(Re^{-2})$  (Duguet et al. 2010) with the new feature being the spanwise localisation of the flow before streak breakdown. A similar investigation has been carried out in the asymptotic suction boundary layer for  $Re$  up to 5000 where a scaling of  $E_c = 0.38Re^{-2}$  is found (Cherubini et al. 2015). This comfortably undercuts earlier estimates using initial conditions based upon: a) random 3-dimensional noise; b) streamwise vortices; c) oblique waves (Levin et al. 2005) and d) two pairs of localised counterrotating vortices (Levin & Henningson 2007): see Figure 9 of Cherubini et al. (2015) for a comparison.

## 4.2. Exploring Other Transition Scenarios

Beyond identifying the minimal seed and its subsequent evolution, other forms of transition generated by larger disturbances can be uncovered using the optimization approach. In a noisy environment, for example, where disturbance levels are much larger than the energy level of the minimal seed, determining optimal routes to turbulence after a (short) time horizon is of more natural concern. This, of course, is just the problem of computing  $E_c(T)$  where  $T$  is finite and, as stressed above, may yield an approximation to the minimal seed or a completely different optimal disturbance which starts off near a different part of the edge, or is substantially removed from it if  $T$  is small enough. A good example of the latter scenario is given by Cherubini & De Palma (2013) who found a bursting form of transition in plane Couette flow by computing small  $T$  energy growth optimals at large  $E_0 > E_{NL}$ : see **Figure 3** and compare the top plots in their Figure 17. In this bursting transition, the flow trajectory leaves the vicinity of the edge along a different unstable manifold than that originating from the edge state, and so follows a different evolution than that of turbulent seeds close to the minimal seed. This new manifold, which emerges from some other state on the edge, plausibly forms a heteroclinic connection to a high energy state buried in the basin of attraction of the turbulent state but not in the attractor itself: see **Figure 4**. A similar phenomenon has been seen in stratified plane Couette flow where an initial burst in energy is a precursor to the turbulent state and persists even when the turbulent state is eventually suppressed by strong stable stratification (Olvera & Kerswell 2017). Farano et al. (2017) have also looked for bursting events using a turbulent mean as the reference state in channel flow. By tuning  $T$  to be the eddy turnover time at an ‘inner’ (in viscous wall units  $y^+ = 19$ ) and ‘outer’ part (the centreline of the channel) of the flow, they find

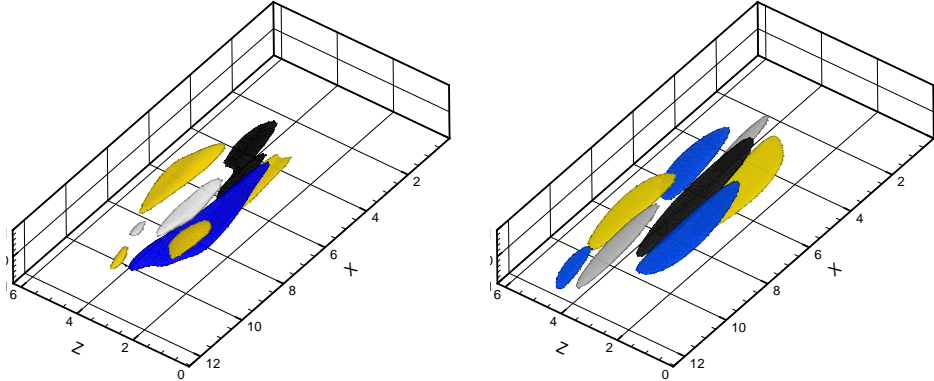


**Figure 3**

Optimals for plane Couette flow (boundary at  $Y = \pm 1$  moving in the  $\pm X$  direction) at  $Re=400$  obtained by nonlinear optimization with  $(E_0, T) = (0.05, 50)$  (left) and  $(0.0027, 300)$  (right) which approximates the minimal seed. Blue/yellow isosurfaces indicate negative/positive streamwise velocity perturbation (contours  $\pm 0.06$  left and  $\pm 0.013$  right) whereas black/light gray ones represent negative/positive spanwise velocity perturbation ( $\pm 0.055$  left and  $w = \pm 0.02$  right). Data courtesy of Cherubini & De Palma (2013).

different bursting optimals which resemble observed large energy events.

Probing the early stages of transition has also been attempted by confining attention to the initial approach to the edge state along its stable manifold. Here an objective functional has been developed which balances minimising the initial energy of the perturbation with the closeness with which it gets to the edge state over a range of  $T$  in plane Couette flow (Cherubini & De Palma 2014b, 2015). The calculated optimal is found to become successively less structured as  $T$  increases until the minimal seed emerges at large times: Figure 5 of Cherubini & De Palma (2015) shows how the energy minimum converges to  $E_c$  for large  $T$ .

In experiments where only specific forms of disturbance can be generated to initiate transition - for example, injecting or removing fluid through small holes in the boundary of pipe flow (Hof et al. 2003, Peixinho & Mullin 2007), the problem of interest is typically to select the most dangerous such disturbance to trigger turbulence and hence estimate  $E_c$ . In this case, the optimization procedure must be adapted to work only over the reduced set of competitor initial conditions. This is easily accomplished by projecting the variational derivative  $\delta\mathcal{L}/\delta\mathbf{u}(\mathbf{x}, 0)$  down onto the subset of allowed disturbances until a revised minimal seed emerges. This has not been done yet but all the ingredients including the successful design of an artificial body forcing to theoretically model the inflow and outflow jets (Mellibovsky & Meseguer 2009) are now available.

### 4.3. Detecting Nearby Saddles

A very similar optimization procedure can be used to explore the neighbourhood in phase space of a (reference) flow state for nearby unstable states as that discussed above for identifying minimal seeds. Providing the objective functional is chosen to be maximised

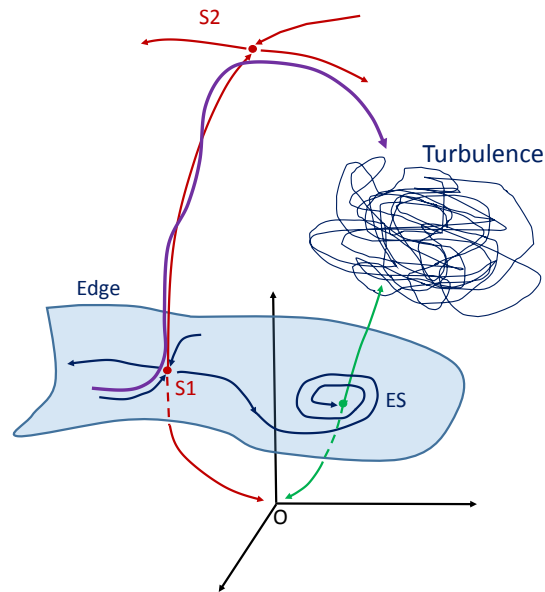


**Figure 4**

A sketch of phase space to illustrate how a different bursting transition scenario (initiated by a disturbance of larger amplitude than the minimal seed) can occur than that which is mediated by the edge state (ES). The reference state is the origin  $O$  of the coordinate system.  $S1$  is a saddle point on the edge (blue surface) and it is its unstable manifold perpendicular to the edge which causes the bursting phenomenon leading the trajectory possibly up to another saddle  $S2$  as shown before it ultimately gets attracted by the the turbulent attractor living at lower energy (energy is depicted here as distance from  $O$ ).

away from the reference state, the optimization procedure will select disturbances from the energy hypersphere which lie nearest to or on the stable manifold of a nearby solution in phase space, if  $T$  is large enough, as this is the best way to avoid converging back into the reference state. The difference now, however, is since the nearby solution is unstable,  $T$  cannot be too large otherwise even these disturbances will have decayed away (realistically it is improbable to stay on the stable manifold to converge in to the unstable state). Once such an optimal disturbance has been found, its temporal evolution will show evidence of a transient approach to the new solution such as a plateauing of the objective functional value in time if the new state is steady. A sufficiently close visit can yield a flow state convergeable using a now-standard Newton-GMRES algorithm into the neighbouring state.

This has recently been demonstrated in wide-box plane Couette flow at low  $Re$  where a multiplicity of states are known to co-exist (Olvera & Kerswell 2017). In particular, the spanwise-localised ‘snake’ solution of Schneider et al. (2010) coexists with repeated copies of the original global solution found by Nagata (1990) in a narrow domain. Not surprisingly, the stable manifold of the ‘snake’ solution passes closer to the basic shear state (in energy norm) than that of Nagata’s solution. However, the latter offers the possibility of greater energy growth as it is global and hence is preferred if reachable from the hypersurface of initial conditions. As a result, there is an energy threshold for which the optimal transiently approaches the snake solution - see **Figure 5** - and a yet higher threshold beyond which

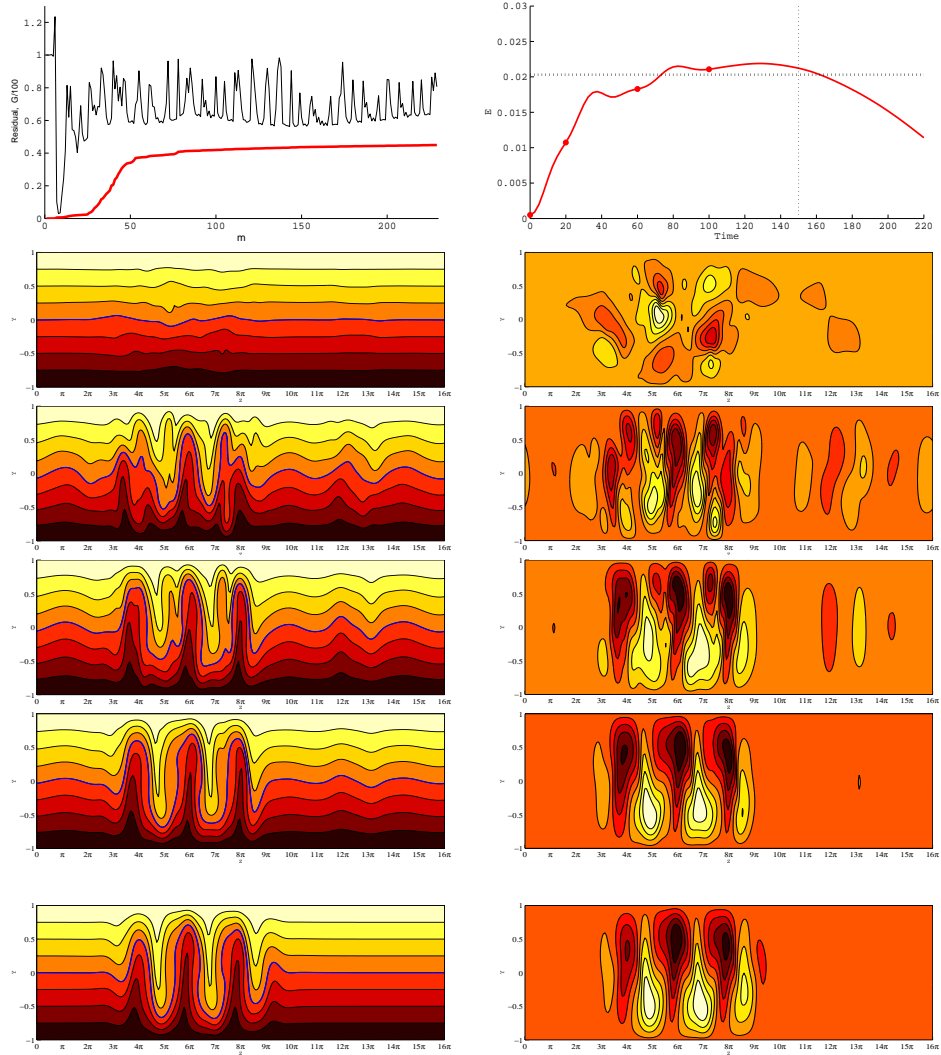


**Figure 5**

Top left: The residual  $:= \int |\delta \mathcal{L} / \delta \mathbf{u}^{(m)}(\mathbf{x}, 0)|^2 dV / \int |\mathbf{u}^{(m)}(\mathbf{x}, 0)|^2 dV$  (black) and the energy gain/100 (bold red) plotted against looping iterations  $m$  for the optimization procedure in plane Couette flow at  $Re = 180$  in a  $4\pi \times 2 \times 16\pi$  domain for  $E_0 = 5 \times 10^{-4}$  and  $T = 150$  (76). Top right: the temporal evolution of the  $m = 200$  iterate (initial condition). Red dots indicate the times ( $t = 0, 20, 60$  and  $100$ ) where cross-sections of the total flow (left: 8 contours across  $[-1, 1]$ ) and flow away from laminar state and right: 8 contours across  $[-0.82, 0.82]$ ) are plotted with time increasing downwards. A dotted horizontal line shows the kinetic energy level of this subsequently converged solution. Bottom: The flow state (left: total flow, and right: perturbation away from the laminar state) converged from using the flow state at  $t = 100$  as an initial guess for a Newton-GMRES algorithm (see Olvera & Kerswell 2017 for details).

Nagata's solution is approached (see §6.3 in Rabin 2013). Figure 5 shows the plateauing in the objective functional over  $t \in [80, 160]$  and snapshots of the evolving flow state. The last flow state shown at  $t = 100$  converges using a Newton-GMRES algorithm to the exact solution shown at the bottom of the figure (Olvera & Kerswell 2017). The procedure works just as well to isolate Nagata's solution.

This approach can be used to look for new solutions in regions of parameter space where little is known. For example, the simple shear state is provably unique in plane Couette flow for  $Re < 20.7$  and provably non-unique for  $Re \geq 127.7$  where Nagata's solution exists. However, a preliminary search has so far found nothing at  $Re = 100$  (Olvera & Kerswell 2017) suggesting that the uniqueness of the simple shear state extends up to here and probably all the way to 127.7.

#### 4.4. Stability of Temporally- and Spatially-Evolving flows

**4.4.1. Spatially-Evolving Flows.** The linear (modal) stability analysis of spatially-evolving flows can either be attempted locally, by assuming the base flow is slowly varying relative to the disturbance being considered, or globally, by considering a large domain and looking for growing global disturbances (e.g. see Chomaz (2005)). With increasing computational power, the latter has naturally become more prevalent although it is still computationally expensive. Nonmodal analysis (linear or nonlinear) can be carried out in either but the time horizon over which energy growth is sought is then restricted by the timescale over which the base flow is seen to vary by the disturbance or the transit time of the flow through the truncated domain. For example, in the Blasius boundary layer calculations of Cherubini et al. (2010), the boundary region studied is  $x \in [200, 400]$ , where the leading edge is at  $x = 0$  and the evolving disturbance is forced to vanish at either end of this domain. The nonlinear optimals which emerge are necessarily positioned near the upstream domain boundary and  $T$  is taken small enough so that disturbance doesn't interact with downstream boundary. Providing this global approach is taken, nonmodal analysis is straightforward to formulate since the starting position of the optimal disturbance emerges as part of the optimization procedure once the exact (spatial) domain of interest has been chosen. For a time-evolving base state situation, however, knowing when to start the optimization procedure - i.e. introduce the disturbance - is a nontrivial consideration and it is to this situation we now turn.

**4.4.2. Time-Periodic States.** In the periodic case, the usual choices for a modal analysis are again local in time - a 'quasi-static' analysis in which the base flow is assumed frozen in time - and a global-in-time formal Floquet analysis. The latter can identify modal energy growth across one period only which repeats to give asymptotically sustained growth. However, there may be strong nonmodal energy amplification of infinitesimal disturbances within a subinterval of a period which happens to decay by the end of the period and/or transient energy growth over multiple periods, both of which can be identified by a linear nonmodal analysis (see §3.3 of Schmid (2007)). Determining at what finite amplitude of disturbance either of these transient effects may trigger transition requires a nonlinear nonmodal stability analysis. Two thresholds can be pursued. The first is for a turbulent state to be triggered within a period (small  $T$ ) but which relaminarises by the end of it and the second, larger threshold is for sustained turbulence which persists once triggered over subsequent periods (large  $T$ ). In the latter, the objective functional may need to be

some sort of a time average of the energy or dissipation rate over the latter part of the time period to keep the variational derivatives relatively smooth when transient turbulence is triggered, but sustained turbulence is not yet been reached (e.g. see Monokrousos et al. 2011).

In either situation, the time origin for the optimization procedure must either be a priori chosen (and then optimised over as done in Rabin et al. 2014) or calculated as part of the optimization procedure. In the latter situation, the Lagrangian (expression (4)) can be rewritten as

$$\mathcal{L} = E(T + T_0) + \lambda \{E(T_0) - E_0\} + \int_{T_0}^{T+T_0} \langle \dots \rangle dt.$$

where  $E(t) := \langle \frac{1}{2} \mathbf{u}(\mathbf{x}, t)^2 \rangle$  is the kinetic energy,  $T_0$  is now a variable time origin relative to the base state and, as before,  $T$  is the time horizon. The Euler-Lagrange equation for  $T_0$  (keeping  $T$  fixed) is then simply

$$\frac{\delta \mathcal{L}}{\delta T_0} = \frac{\partial E}{\partial t} \Big|_{T+T_0} + \lambda \frac{\partial E}{\partial t} \Big|_{T_0} \quad (19)$$

(assuming that the Navier-Stokes equation and incompressibility are imposed at  $T_0$  and  $T_0 + T$ ) which can be straightforwardly incorporated in the looping algorithm. Here  $\delta \mathcal{L} / \delta T_0$  is evaluated at the end of a loop (when both  $\mathbf{u}(\mathbf{x}, T_0)$  and  $\mathbf{u}(\mathbf{x}, T_0 + T)$  are available) and then used to move  $T_0$  in the direction of increasing  $\mathcal{L}$  for the next loop ( $\mathbf{u}(\mathbf{x}, T_0)$  is then used to initiate the next loop at this new time). Rabin et al. (2012) experimented with optimising  $T$  (keeping  $T_0 = 0$ ) in plane Couette flow when looking for the minimal seed but found that  $T$  could become small caused by short term transients which complicated the results.

An outstanding example of where this analysis could be useful is Stokes' second problem of an oscillating plate bounding a semi-infinite ( $y \geq 0$ ) fluid-filled domain. There the base flow is

$$U(y, t) = \cos(2\pi t - \sqrt{\pi} y) e^{-\sqrt{\pi} y} \quad (20)$$

where the period of oscillation  $T$  and diffusive length scale  $\sqrt{\nu T}$  are used as units of time and length respectively ( $\nu$  being the kinematic viscosity). Defining a Reynolds number as  $Re := U \sqrt{T} / \nu$  where  $U$  is the maximum speed of the oscillating plate (after Biau 2016), a quasi-static linear analysis gives an estimate of the critical  $Re$  as 152 for linear instability whereas a (proper) Floquet analysis gives a figure of 2511 (see Ozdemir et al. 2014 for references). The actual transitional  $Re$ , however, is firmly in the middle of these theoretical estimates at about 900, indicating a finite-amplitude instability. A recent (linear) nonmodal analysis reveals that infinitesimal disturbances can experience huge energy growth - e.g. a growth factor of  $3.8 \times 10^6$  at  $Re = 1000$  (see Table 1 of Biau 2016) - over a sub-interval of an oscillation through the Orr mechanism, suggesting that the (finite) energy thresholds for partial or sustained turbulence may be very small. This would imply that the finite amplitude instability can be triggered very easily in both experiments by ambient noise and numerical simulations by the supposedly small initial conditions used to initiate runs (Ozdemir et al. 2014). The linear nonmodal analysis also indicates that only the Orr mechanism is important and so the optimal starting time found there may be good for the nonlinear nonmodal analysis too: see Table 1 of Biau (2016).

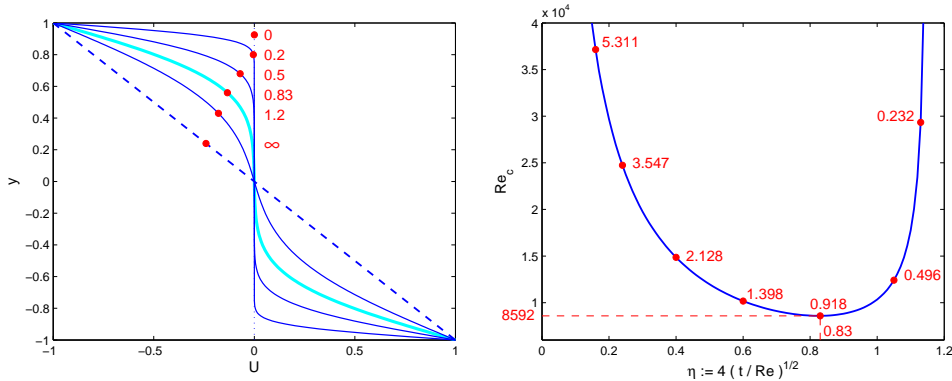


**Figure 6**

The base flow and linear stability results for impulsively started plane Couette flow. Left: the base flow  $u(y, \eta)$  plotted against  $y$  for a selection of  $\eta$  (labels on curves) ( $u(y, \eta) \rightarrow -y\hat{x}$  as  $\eta \rightarrow \infty$ ). Right: the neutral curve obtained by solving the Orr-Sommerfeld equation assuming the quasi-static (frozen-base state) approximation. The labels near the curve indicate the values of the critical streamwise wavenumber at the dots on the curve). The lowest Reynolds number for linear instability is  $Re = 8592$  at  $\eta = 0.83$  where the critical streamwise wave number is 0.918.

**4.4.3. Non-Periodic Time-Evolving States.** For a non-periodic time-evolving state, linear modal stability analysis doesn't make much sense, except in the approximate quasi-static limit which assumes that the base flow is evolving slowly compared to the disturbance being considered. Linear and nonlinear nonmodal analysis, however, can be straightforwardly applied using the looping approach with the latter allowing minimal disturbances to be targeted which reach specific endstates. A simple example is impulsively-started plane Couette flow which is the flow between two parallel plates at  $y = \pm 1$  and driven by their differential velocities  $\mp H(t)\hat{x}$  where  $H(t)$  is the Heaviside function ( $= 0$  for  $t < 0$  and  $= 1$  for  $t \geq 0$ ). The time evolving base state can be expressed as

$$u(y, \eta) := \sum_{n=0}^{\infty} \operatorname{erfc} \left[ \frac{2}{\eta} (y + 2n + 1) \right] - \sum_{n=0}^{\infty} \operatorname{erfc} \left[ \frac{2}{\eta} (2n + 1) \right] - \sum_{n=1}^{\infty} \operatorname{erfc} \left[ \frac{2}{\eta} (-y + 2n - 1) \right] + \sum_{n=1}^{\infty} \operatorname{erfc} \left[ \frac{2}{\eta} (2n - 1) \right]$$

with  $\eta := 4\sqrt{t/Re}$  and  $Re := Uh/\nu$ , where  $2U$  is the differential speed between the plates,  $2h$  the distance between the plates and  $\nu$  the kinematic viscosity (Schlichting 1955): see **Figure 6(a)**. Quasi-static linear stability analysis indicates a critical Reynolds number which decreases from infinity as time increases from 0 to a minimum of 8592 at approximately  $t = t_c \approx (0.83/4)^2 Re$  and increases again to infinity with time: see **Figure 6(b)**. Since the critical  $Re$  increases back to infinity at large times (developed plane Couette flow is linearly stable), developing plane Couette flow in fact has to be linearly stable: any growing infinitesimal disturbance from early times has to ultimately decay at long times. Nevertheless, the quasi-static results have worth. Firstly, they open up the possibility of branch continuing solutions in  $t$  away from the developing solution when bifurcations exist for  $Re > 8592$  (see Deguchi & Walton 2013 for an application in developing pipe flow). Secondly, they pose an interesting stability question about the start-up process: how easy

is it to influence the endstate reached via a finite-amplitude disturbance after a certain time when there are multiple attractors? This is a generalised minimal seed question since the time of disruption as well as the optimal disturbance must be sought to minimally disturb the evolving simple shear state to an alternate attractor (e.g. turbulence at high  $Re$ ). In the first instance, if only one alternative attractor is present (the generic situation in plane Couette flow at high enough  $Re$ ), using the final energy of the disturbance away from the simple shear state as the objective functional should work provided a ‘long’ time horizon  $T$  is chosen. The time-evolving mixing layer (e.g. Arratia et al. 2013) is another good example of where this approach may be used profitably.

## 5. Other Applications

### 5.1. Weather Forecasting and Sensitivity

In weather forecasting, an important issue is the short time behaviour of a predictive model initiated with imperfect initial data (the state of the atmosphere is never known everywhere at once). Understanding the sensitivity of the model to errors in the initial data is then paramount for assessing the subsequent errors in forecasts. Ensemble forecasts (Palmer et al. 1993, Buizza & Palmer 1995) attempt to estimate the likely uncertainty in the forecast by considering an ensemble of runs initiated with data polluted by the most ‘dangerous’ errors. These most dangerous errors are taken to be the singular value vectors or nonmodal (linear) optimals calculated from the linear operator based upon the unpolluted prediction and are then assigned some finite amplitude. There have been attempts to incorporate nonlinearity into this by an iterative approach (Oortwijn and Barkmeijer 1995, Barkmeijer 1996) as well as a fully nonlinear approach (Mu 2000, Mu et al. 2003, Mu & Zhang 2006, Mu & Jiang 2008a,b, Mu et al. 2010, Duan & Zhou 2013, Jiang et al. 2013, Ziqing et al. 2013, Dijkstra & Viebahn 2015). Of key concern is that given the amplitude of perturbation assumed, fully nonlinear optimals may indicate a completely different response of the system compared to the linear optimals precisely because the perturbation is finite amplitude. This will then have implications for the probability distribution of what the true forecast is some given time later.

Mu and coworkers have also computed nonlinear optimals - or ‘conditional nonlinear optimal perturbation’ (CNOP) in their words - to study the sensitivity of other weather and climate events such as El Niño events (Yu et al. 2009, Duan et al. 2013, Mu et al. 2013), ‘blocking’ onsets (Mu & Jiang 2008b, 2011 and Jiang & Wang 2010) and the Kuroshio large meander (Wang et al. 2012, 2013), and to probe nonlinear stability of simple oceanographic models (Mu et al. 2004, Mu & Zhang 2006). In their first study, Mu et al. (2004) considered a very simple (2-dimensional ODE) box model of the thermohaline circulation but subsequent work (Mu & Zhang 2006) scaled this effort up to a 2-dimensional quasigeostrophic model with 512 grid points. van Scheltinga & Dijkstra’s (2008) model of a double-gyre ocean circulation, which uses 4800 degrees of freedom, represents the most ambitious application so far in this context. Given that the Navier-Stokes equation discretised using millions of degrees of freedom has now been handled successfully in the transition to turbulence context, there is clearly an opportunity to push this work further.

## 5.2. Thermoacoustics

The optimization approach to identify the critical disturbance of one linearly-stable state so that another state is reached has also been used in thermoacoustics. Juniper (2011a,b) has studied the horizontal Rijke tube, which is modelled by a couple of 1-space 1-time PDEs, using this approach. Here the laminar state is a fixed point, the edge state is an unstable periodic orbit and the ‘turbulent’ state is a stable periodic orbit (respectively the ‘lower’ and ‘upper’ branches which emerge from a saddle node bifurcation). The Rijke tube system is sufficiently simple that an exhaustive study of optimal energy growth can be carried out over both amplitude and time horizon  $T$  to confirm the predictions of the nonlinear optimization procedure (Juniper 2011b).

## 5.3. Magnetic Field Generation and Mixing in Stratified flows

Two very different applications have been attempted following the success of the nonlinear looping approach in the transition problem. In 2012, Willis considered the kinematic dynamo problem in magnetohydrodynamics, which asks the question of whether a magnetic field  $\mathbf{B}$  can grow on a velocity field  $\mathbf{u}$  in an electrically conducting fluid. This is usually formulated by assuming a specific form for the velocity field and then converting the induction equation for the magnetic field into an eigenvalue problem. However, Willis (2012) formulated a novel optimization problem to both identify the magnetic field and velocity field which together give the largest magnetic field growth for a given magnetic Reynolds number  $R_m$ . The only constraints on the velocity field are incompressibility, periodicity (calculations are performed in a triply periodic box) and fixed energy dissipation rate (or, equivalently, fixed power input) so that the Lagrangian is

$$\begin{aligned} \mathcal{L} = & \langle \mathbf{B}_T^2 \rangle - \lambda_1 (\langle (\nabla \times \mathbf{u})^2 \rangle - 1) - \lambda_2 (\langle \mathbf{B}_0^2 \rangle - 1) - \langle \Pi_1 \nabla \cdot \mathbf{u} \rangle - \langle \Pi_2 \nabla \cdot \mathbf{B}_0 \rangle \\ & - \int_0^T \langle \mathbf{\Gamma} \cdot \left[ \frac{\partial \mathbf{B}}{\partial t} - \nabla \times (\mathbf{u} \times \mathbf{B}) - \frac{1}{R_m} \nabla^2 \mathbf{B} \right] \rangle dt \quad (21) \end{aligned}$$

where  $\mathbf{B}_0$  is the initial magnetic field,  $\mathbf{B}_T$  the final magnetic field at  $t = T$  and  $\lambda_i$ ,  $\Pi_i$  and  $\mathbf{\Gamma}$  are Lagrange multipliers. In this formulation, the induction equation is now fully nonlinear since both  $\mathbf{B}$  and  $\mathbf{u}$  are unknowns. This work has been extended to finite fluid-filled domains which adds the extra complication of matching the magnetic field to surrounding (external) conditions (Chen et al. 2015).

In 2-dimensional channel flow, Foures et al. (2014) have identified initial velocity fields  $\mathbf{u}(\mathbf{x}, t)$  which lead to ‘maximal’ mixing of a passive scalar  $\theta(\mathbf{x}, t)$  depending on exactly how this mixing is quantified. The scalar is initially arranged in two unmixed layers of different concentrations meeting at the midplane of the channel and a number of different objective functionals

$$\mathcal{L} := \frac{1}{2}(1 - \alpha) \int_0^T \langle \mathbf{u}(\mathbf{x}, t)^2 \rangle dt + \frac{1}{2} \alpha \langle |\nabla^{-\beta} \theta(\mathbf{x}, T)|^2 \rangle \quad (22)$$

extremised using the nonlinear looping approach. Optimal initial velocity conditions which maximise the time-averaged energy ( $\alpha = 0$ ), minimise the variance of the passive scalar ( $\alpha = 1$ ,  $\beta = 0$ ) or minimise the ‘mix-norm’ of the scalar ( $\alpha = 1$ ,  $\beta = 1$ ) are each tested to see how effective their subsequent evolution is in mixing up the scalar field.

## 5.4. Control

Once the nonlinear stability of a given flow has been quantified by identifying the critical disturbance energy and structure, it becomes feasible to attempt to design a more (or less) nonlinearly stable flow by changing some aspect of the system. Rabin et al. (2014) tried just this in plane Couette flow by adding an extra spanwise oscillation (amplitude  $A$  and frequency  $\omega$ ) of both boundaries to their relative motion so that the boundary motion at  $y = \pm 1$  is

$$\mathbf{u}(x, \pm 1, z, t) = \mp \hat{\mathbf{x}} + A \sin(\omega t) \hat{\mathbf{z}} \quad (23)$$

(using the set-up of §4.4.3). This modified boundary motion leads to the revised basic flow response  $\mathbf{u}_A(\mathbf{x}, t; A, \omega, Re)$  and the question is then: can  $A$  and  $\omega$  be chosen such that  $\mathbf{u}_A$  is more nonlinearly stable (where ‘more stable’ means the energy of the critical disturbance to reach the basin boundary,  $E_c$ , is increased)? As the reference state is time-periodic, the nonlinear nonmodal analysis is more intensive as an extra search has to be conducted over the exact time within a period when the disturbance is introduced. Despite this extra overhead, Rabin et al. (2014) show that there is a sweet spot in the  $(A, \omega)$  plane where the flow  $\mathbf{u}_A$  can be made 41% more stable than the unoscillated basic flow at  $Re = 1000$  (i.e.  $E_c$  is  $1.41 \times$  the uncontrolled value). The implication is that if the ambient noise level is between the unoscillated and oscillated values, there are power savings to be had since  $\mathbf{u}_A$  will be stable to the noise while the unoscillated system should be turbulent and therefore consume much more power. This is very much a proof-of-concept computation in that 1) no robustness of the the sweet spot over  $Re$  was demonstrated and, more seriously, 2) the optimization approach assumes the introduction of one disturbance only and its subsequent evolution rather than a continual stream of disturbances. This latter assumption can be lifted by opening up the optimization to multiple disturbances distributed over the time interval  $[0, T]$  but then the exact amplitude condition to constrain different disturbance patterns is less clear (Lecoanet & Kerswell 2013). For example, the energy of two identical disturbances occurring at different times is half the energy measure if the two disturbances occur simultaneously. This is, however, an interesting direction for further work.

Other work stimulated by the recent success of nonlinear looping is that of Passaggia and Ehrenstein (2013) who have looked at controlling the 2-dimensional boundary layer dynamics over a bump by blowing and sucking using the full Navier-Stokes equation. This has been extended to 3 dimensions by Cherubini et al. (2013) where the linear and nonlinear optimals have been used as initial conditions. This work remains a long way off real applications because it relies on knowing the state of the system at each time and performing costly optimization calculations, which can’t be done in real time, so the use of fully nonlinear methods in control are still impractical (e.g. Joslin et al. 1995, 1997, Gunzburger 2000, Bewley et al. 2001, Chevalier et al. 2002, Pralits et al. 2002, Kim & Bewley 2007).

## 6. Summary and Future Directions

This article has described a new optimization technique for analysing the nonlinear stability of a reference state. This is ostensibly for a linearly stable state and then the fundamental question is: what sort of disturbance will shift the system beyond the state’s basin of attraction? However, it can also be useful for linearly unstable states if the timescale of the linear instability is much longer than the time horizon of interest (e.g. in Blasius boundary layer flow). Then ‘bypass’ processes acting on shorter timescales can be analysed as if the

reference state is stable. The core of the approach is to ‘nonlinearise’ nonmodal analysis so that competing disturbances of a given fixed finite amplitude are considered to optimise an objective functional, constrained by the fact that each disturbance evolves subject to the full Navier-Stokes equation. The discussion has focussed on the final energy growth of the disturbance mostly for simplicity and historical reasons, but in fact this is a sensible default choice for most applications because the asymptotic limit of disturbance energy clearly signals whether the disturbance started inside, on or outside the basin boundary of the reference state.

As stated earlier, the idea to extend nonmodal analysis to treat finite amplitude disturbances is not particularly profound. Neither is the observation that the optimal value of the objective functional will undergo a sudden change to larger values as the initial disturbance amplitude is increased beyond the point where some can explore parts of phase space beyond the basin of attraction. Instead, what is noteworthy is the recent realisation that the fully nonlinear non-convex optimization problem so formulated can actually be solved using a direct-adjoint looping approach on large degree-of-freedom systems to give credible results. Conceptually, this procedure provides a theoretical bridge between the two complementary perspectives of linear nonmodal analysis (which technically includes linear stability analysis if  $T \rightarrow \infty$ ) and the (nonlinear) dynamical systems approach to fluid mechanics. The strict inclusion of nonlinearity means the approach is necessarily computational and has its uncertainties (e.g. identifying global over local optimals). However, the fact that the nonlinear optimals which have emerged so far appear to be as a concatenation of linear processes hints that a simpler semi-analytical framework could be available (e.g. see Pralits et al. 2015 for some work in this direction).

This article has also tried to indicate how flexible this optimization approach is. Although the focus has been on bistable systems, multistable situations can be handled providing the objective functional is designed to pick out the desired target state. A long-lived transient state can also be targeted which is actually what was originally treated since the turbulence in shear flows at low Reynolds number and in constrained computational domains tends only to be a chaotic repeller (e.g. the short periodic pipe of Pringle & Kerswell 2010). Some preliminary work using nonlinear nonmodal analysis has also been described to probe phase space for unstable solutions nearby to the reference state (Olvera & Kerswell 2017).

The technique as described here specifically considers only one finite-amplitude disturbance and then considers its evolution in the absence of any further disturbances. This is sufficient to gauge the nonlinear stability of the reference state but, in practice, flows can be exposed to multiple, if not a continuous stream, of disturbances and how these interact to push the system to another attractor is more important. The optimization approach can be straightforwardly extended to consider multiple disturbances distributed across an interval and there is an interesting connection to be made with the continuously disturbed or ‘noisy’ situation (Freidlin & Wentzell 1998, Waugh & Juniper 2011, Wang et al. 2015, Lecoanet & Kerswell 2017).

A number of areas ripe for future development have also been discussed. Perhaps most obvious is the treatment of time-periodic states. The procedure is more arduous in this case - an extra optimization over the disturbance time is required - but still doable and the easier linear calculation may suggest a shortcut through this. Some aperiodic flows like an impulsively started flow or the diffusing mixing layer situation can also be treated in the same way, where the optimal time to add the disturbance can be narrowed down by a

linear quasi-static analysis. However, it is presently unclear how to handle reference states which are quasi-periodic or even chaotic and a more natural approach would be to consider noise instead. Another area is ‘design’. The ability to quantify the nonlinear stability of a state opens up the possibility of manipulating the system to produce a ‘better’ flow, whether this be more or less stable. This idea has been briefly explored by actively (using more power) modifying the motion of the boundaries in plane Couette flow but there are interesting passive options (requiring no additional power) such as adjusting the shape of the boundaries to be explored. The technique can also be used to help design experiments where typically a limited suite of perturbations are available to the experimentalist. The search for an optimal disturbance to trigger a desired effect (e.g. transition or a large amplitude event) can then be simply restricted to those which are practical, avoiding a trail-and-error approach.

In conclusion, nonlinear nonmodal analysis appears to be a valuable tool to probe the dynamics around a given reference state. Coupled to a search over the amplitude of the competing disturbances, a computational tool emerges to probe basin boundaries and, if the ‘other’ state is turbulence, the transition problem. Challenges exist to lessen the computational overhead and perhaps even to make part of the procedure semi-analytic, but with ever-increasing computational power, it’s hard not to envisage this technique becoming a standard theoretical tool in fluid mechanics.

#### SUMMARY POINTS

1. Nonlinear nonmodal analysis. It is now feasible to identify a disturbance of a given initial (finite) amplitude to a reference state which maximises the energy growth some time later using an iterative direct-adjoint looping procedure thereby extending (linear) nonmodal analysis. This has recently been performed for flow systems with millions of degrees of freedom, is easily extendable to treat other objective functionals and can be used to investigate phase space beyond that which immediately surrounds the reference state.
2. Nonlinear nonmodal stability analysis. Providing the objective functional to be maximised is chosen so that it takes heightened values at the new attracting target state, nonlinear nonmodal analysis can be coupled with a search over disturbance amplitude to identify the critical disturbance which corresponds to the closest point of approach of the basin boundary to the reference state. For the transition problem, this critical disturbance is called the minimal seed for transition and is arbitrarily close to initial conditions beyond the basin boundary which lead to turbulence.
3. Bridging a gap. Nonlinear nonmodal stability analysis bridges the conceptual gap between (linear) nonmodal stability theory which focusses on the behaviour in the immediate neighbourhood of a reference state and the (fully nonlinear) dynamical systems approach to fluid mechanics. By identifying the critical disturbance for a given amplitude measure, the nonlinear stability of a flow state can now be quantified which can then be used to design a more stable or less stable state.
4. Flexibility. The general approach is one of optimization of a chosen objective func-

tional subject to constraints which include the full Navier-Stokes equations and is therefore incredibly flexible. The nonlinear stability of time-evolving reference states can be considered as can optimal starting conditions identified which lead to desired flow episodes (e.g. large energy events such as ‘bursting’ or transition by a certain time).

## FUTURE ISSUES

1. Convergence. Implementations of nonlinear nonmodal analysis sometimes show stalling convergence even though a reasonable optimal still appears to emerge. Work is needed to understand this and to improve the update procedure for the optimal in the direct-adjoint looping iterations. Currently there is no specific tailoring of this procedure to the likely form of the optimal (e.g. the NLOP is generically fully localised in space) or for what initial conditions can be generated in the laboratory.
2. Multiple disturbances. This article discusses the implications of applying a single disturbance to a flow system and then studying its subsequent evolution free of any further disturbances. While useful for formally assessing the nonlinear stability of the reference state, this is less relevant to a reference state continually being exposed to disturbances. Multiple disturbances can be handled using the optimization approach of this article and connecting this with the continuous noise limit (large deviation theory and ‘instantons’) is an interesting future direction.
3. Applications. The most obvious new direction for applications is the treatment of time-dependent reference states. Even the simplest scenario of a time-periodic state leads to a more involved optimization procedure since the application time for the disturbance ostensibly needs to be optimized over. Avoiding this extra search by exploiting some physical insight as, for example, provided by the (linear) nonmodal analysis over short times would represent a valuable step forward.
4. Design. The ability to quantify the nonlinear stability of a given flow state opens up the possibility of then subsequently manipulating or designing a ‘better’ system whether this means one with a more or less stable reference state. So far only one proof-of-concept calculation has been done by introducing an extra motion of the boundary so developing this idea further (e.g. to include boundary shape design) is an exciting direction for future work.

## DISCLOSURE STATEMENT

The author is not aware of any affiliations, memberships, funding, or financial holdings that might be perceived as affecting the objectivity of this review.

## ACKNOWLEDGEMENTS

I'd like to thank Stefania Cherubini, Jake Langham and Jacob Page for commenting on an early version of the manuscript. Thanks also to Chris Pringle, Stefania Cherubini (again) and Daniel Olvera for helping to produce Figures, 2, 3 and 5 respectively.

## LITERATURE CITED

- Arratia C, Caulfield CP, Chomaz J-M. 2013. Transient perturbation growth in time-dependent mixing layers. *J. Fluid Mech.* **717**:90–133
- Andersson P, Berggren M, Henningson DS. 1999. Optimal disturbances and bypass transition in boundary layers. *Phys. Fluids* **11**:134–150
- Barkmeijer J. 1996. Constructing fast-growing perturbations for the nonlinear regime. *J. Atmos. Sci.* **53**:2838–2851
- Berggren M. 1998. Numerical solution of a flow-control problem: vorticity reduction by dynamic boundary action. *Siam J. Sci. Comput.* **19**:829–860
- Bewley TR, Moin P, Temam R. 2001. DNS-based predictive control of turbulence: an optimal benchmark for feedback algorithms. *J. Fluid Mech.* **447**:179–225
- Biau D. 2016. Transient growth of perturbations in Stokes oscillatory flows. *J. Fluid Mech.* **794**:R4
- Boberg L, Brosa U. 1988. Onset of turbulence in a pipe. *Z. Naturforsch.* **43a**:697–726
- Buizza R, Palmer TN. 1995. The singular-vector structure of the atmospheric global circulation. *J. Atmos. Sci.* **52**:1434–1456
- Butler KM, Farrell BF. 1992. 3-Dimensional optimal perturbations in viscous shear-flow. *Phys. Fluids* **4**:1637–1650
- Chen L, Herreman W, Jackson A. 2015. Optimal dynamo action by steady flows confined to a cube. *J. Fluid Mech.* **783**:23–45
- Cherubini S, De Palma P, Robinet J-C, Bottaro A. 2010. Rapid path to transition via nonlinear localised optimal perturbations in a boundary layer flow. *Phys. Rev. E* **82**: 066302
- Cherubini S, De Palma P, Robinet J-C, Bottaro A. 2011. The minimal seed of turbulent transition in the boundary layer. *J. Fluid Mech.* **689**:221–253
- Cherubini S, De Palma P, Robinet J-C, Bottaro A. 2012. A purely nonlinear route to transition approaching the edge of chaos in a boundary layer. *Fluid Dynam. Res.* **44**:031404
- Cherubini S, De Palma P. 2013. Nonlinear optimal perturbations in a Couette flow: bursting and transition. *J. Fluid Mech.* **716**:251–279
- Cherubini S, Robinet J-C, De Palma P. 2013a. Nonlinear control of unsteady finite-amplitude perturbations in the Blasius boundary-layer flow. *J. Fluid Mech.* **737**:440–465
- Cherubini S, De Palma P. 2014a. Minimal perturbations approaching the edge of chaos in a Couette flow. *Fluid Dynam. Res.* **46**:041403
- Cherubini S, De Palma P. 2014b. Minimal-energy perturbations rapidly approaching the edge state in Couette flow. *J. Fluid Mech.* **746**:572–598.
- Cherubini S, De Palma P, Robinet J-C. 2015. Nonlinear optimals in the asymptotic suction boundary layer: transition thresholds and symmetry breaking. *Phys. Fluids* **27**:034108.
- Chevalier M, Högberg M, Berggren M, Henningson DS. 2002. Linear and nonlinear optimal control in spatial boundary layers. *AIAA paper 2002–2755* 3rd Theoretical Fluid Mechanics Meeting, St Louis, Missouri
- Chomaz J-M. 2005. Global instabilities in spatially developing flow: Non-normality and nonlinearity. *Ann. Rev. Fluid Mech.* **37**:357–392
- Corbett P, Bottaro A. 2000. Optimal perturbations for boundary layers subject to streamwise pressure gradient. *Phys. Fluids* **12**:120–130
- Deguchi K, Walton AC. 2013. A swirling spiral wave solution in pipe flow. *J. Fluid Mech.* **737**:R2
- Dijkstra H, Viebahn JP. 2015. Sensitivity and resilience of the climate system: a conditional non-

- linear optimization approach. *Commun. Nonlinear Sci. Numer. Simulat.* **22**:13–22
- Duan W, Yu Y, Xu H, Zhao P. 2013. Behaviors of nonlinearities modulating the El Niño events induced by optimal precursory disturbances. *Clim. Dyn.* **40**:1399–1413
- Duan W, Zhou F. 2013. Non-linear forcing singular vector of a two-dimensional quasi-geostrophic model. *Tellus* **65**:18452
- Duguet Y, Willis AP, Kerswell RR. 2008. Transition in pipe flow: the saddle structure on the boundary of turbulence. *J. Fluid Mech.* **613**:255–274
- Duguet Y, Brandt L, Larsson BRJ. 2010. Towards minimal perturbations in transitional plane Couette flow. *Phys. Rev. E* **82**:026316
- Duguet Y, Monokrousos A, Brandt L, Henningson DS. 2013. Minimal transition thresholds in plane Couette flow. *Phys. Fluids* **25**:084103
- Eaves TS, Caulfield CP. 2015. Disruption of SSP/VWI states by a stable stratification. *J. Fluid Mech.* **784**:548–564
- Eckhardt B, Schneider T M, Hof B, Westerweel J. 2007. Turbulence transition in pipe flow. *Ann. Rev. Fluid Mech.* **39**:447–468
- Farano M, Cherubini S, Robinet J-C, De Palma P. 2015. Hairpin-like optimal perturbations in plane Poiseuille flow. *J. Fluid Mech.* **775**:R2
- Farano M, Cherubini S, Robinet J-C, De Palma P. 2016. Subcritical transition scenarios via linear and nonlinear localized optimal perturbations in plane Poiseuille flow. *Fluid Dynam. Res.* **46**:061409
- Farano M, Cherubini S, Robinet J-C, De Palma P. 2017 Optimal bursts in turbulent channel flow. *J. Fluid Mech.* **817**:35–60
- Farrell BF. 1988. Optimal excitation of perturbations in viscous shear flow. *Phys. Fluids* **31**:2093–2101
- Freidlin MI, Wentzell AD. 1998. *Random Perturbations of Dynamical Systems*. New York: Springer-Verlag
- Foures DPG, Caulfield CP, Schmid PJ. 2014. Optimal mixing in two-dimensional plane Poiseuille flow at high Péclet number. *J. Fluid Mech.* **748**:241–277.
- Guégan A, Schmid PJ, Huerre P. 2006. Optimal energy growth and optimal control in swept Hiemenz flow. *J. Fluid Mech.* **566**:11–45
- Gunzburger M. 2000. Adjoint equation-based methods for control problems in incompressible, viscous flows. *Flow, Turbulence and Combustion* **65**:249–272
- Gustavsson LH. 1991. Energy growth of 3-dimensional disturbances in plane Poiseuille flow. *J. Fluid Mech.* **224**:241–260
- Henningson DS, Reddy SC. 1994. On the role of linear mechanisms in transition to turbulence. *Phys. Fluids* **6**:1396–1398
- Hinze M, Walther A, Sternberg J. 2006. An optimal memory-reduced procedure for calculating adjoints of the instationary Navier-Stokes equations. *Optim. Control Appl. Methods* **27**:19–40.
- Hof B, Juel A, Mullin T. 2003. Scaling of the turbulence transition in pipe flow. *Phys. Rev. Lett.* **91**:244502
- Jiang Z, Wang D. 2010. A study on precursors to blocking anomalies in climatological flows by using conditional nonlinear optimal perturbations. *Quart. J. Roy. Meteor. Soc.* **136**:1170–1180
- Jiang ZN, Mu M, Luo DH. 2013. A study of the North Atlantic Oscillation using conditional nonlinear optimal perturbation. *J. Atmos. Sci.* **70**:855–875
- Joslin RD, Gunzburger MD, Nicolaides RA, Erlebacher G, Hussaini MY. 1995. Self-contained automated methodology for optimal flow control. *Institute for Computer Applications in Science and Engineering (ICASE)* technical report, 95–64
- Joslin RD, Gunzburger MD, Nicolaides RA, Erlebacher G, Hussaini MY. 1997. Self-contained automated methodology for optimal flow control validated for transition delay. *AIAA Journal* **35**:816–824
- Juniper MP. 2011a. Triggering in the horizontal Rijke tube: non-normality, transient growth and

- bypass transition. *J. Fluid Mech.* **667**:272–308
- Juniper MP. 2011b. Transient growth and triggering in the horizontal Rijke tube *Int. J. Spray and Combustion Dynamics* **3**:209–224
- Kawahara G, Uhlmann M, van Veen L. 2012. The significance of simple invariant solutions in turbulent flows. *Ann. Rev. Fluid Mech.* **44**:203–225
- Kerswell RR. 2005. Recent progress in understanding the transition to turbulence in a pipe. *Nonlinearity* **18**:R17–R44
- Kerswell RR, Pringle CCP, Willis AP. 2014. An optimization approach for analysing nonlinear stability with transition to turbulence in fluids as an exemplar. *Rep. Prog. Phys.* **77**:085901
- Kim J, Bewley TR. 2007. A linear systems approach to flow control. *Ann. Rev. Fluid Mech.* **39**:383–417
- Lecoanet D, Kerswell RR. 2013. Nonlinear optimization of multiple perturbations and stochastic forcing of subcritical ODE systems. *Bull. Am. Phys. Soc.* **58**:L10.4
- Lecoanet D, Kerswell RR. 2017. Connection between nonlinear energy growth and instantons. *preprint*
- Levin O, Davidsson EN, Henningson DS. 2005. Transition thresholds in the asymptotic suction boundary layer. *Phys. Fluids* **17**:114104
- Levin O, Henningson DS. 2005. Turbulent spots in the asymptotic suction boundary layer. *J. Fluid Mech.* **584**:397–413
- Luchini P, Bottaro A. 1998. Görtler vortices: a backward-in-time approach to the receptivity problem. *J. Fluid Mech.* **363**:1–23
- Luchini P. 2000. Reynolds-number-independent instability of the boundary layer over a flat surface: optimal perturbations. *J. Fluid Mech.* **404**:289–309
- Luchini P, Bottaro A. 2014. Adjoint equations in stability analysis. *Ann. Rev. Fluid Mech.* **46**:493–517
- Mellibovsky F, Meseguer A. 2009. Critical threshold in pipe flow transition. *Phil. Trans. R. Soc. A* **467**:545–560
- Mellibovsky F, Meseguer A, Schneider TM, Eckhardt B. 2009. Transition in localized pipe flow turbulence. *Phys. Rev. Lett.* **103**:054502
- Monokrousos A, Bottaro A, Brandt L, Di Vita A, Henningson DS. 2011. Nonequilibrium thermodynamics and the optimal path to turbulence in shear flows. *Phys. Rev. Lett.* **106**:134502
- Mu M. 2000. Nonlinear singular vectors and nonlinear singular values. *Sci. China* **43D**:375–385
- Mu M, Duan WS, Wang B. 2003. Conditional nonlinear optimal perturbation and its applications. *Nonlin. Processes Geophys.* **10**:493–501
- Mu M, Sun L, Dijkstra HA. 2004. The sensitivity and stability of the ocean’s thermohaline circulation to finite-amplitude perturbations. *J. Phys. Ocean.* **34**:2305–2315
- Mu M, Zhang Z. 2006. Conditional nonlinear optimal perturbations of a two-dimensional quasi-geostrophic model. *J. Atmos. Sci.* **63**:1587–1604
- Mu M, Jiang ZN. 2008a. A new approach to the generation of initial perturbations for ensemble prediction using dynamically conditional perturbations. *Chinese Sci. Bull.* **53**:2062–2068
- Mu M, Jiang Z. 2008b. A method to find perturbations that trigger blocking onset: conditional nonlinear optimal perturbations. *Am. Meteor. Soc.* **65**:3935–3946
- Mu M, Duan W, Wang Q, Zhang R. 2010. An extension of conditional optimal perturbation approach and its applications. *Nonlin. Proc. Geophys.* **17**:211–220
- Mu M, Jiang Z. 2011. Similarities between optimal precursors that trigger the onset of blocking events and optimally growing initial errors in onset prediction. *J. Atmos. Sci.* **68**:2860–2877
- Mu M, Yu Y S, Xu H, Gong TT. 2013. Similarities between optimal precursors for ENSO events and optimally growing initial errors in El Niño predictions. *Theor. Appl. Climatol.* **115**:461–469
- Nagata M. 1990. 3-dimensional finite-amplitude solutions in plane Couette flow - bifurcation from infinity. *J. Fluid Mech.* **217**:519–527
- Ozdemir CE, Hsu T-J, Balachandar S. 2014. Direct numerical simulations of transition and turbu-

- lence in smooth-walled Stokes boundary layer. *Phys. Fluids* **26**:045108
- Oortwijn J, Barkmeijer J. 1995. Perturbations that optimally trigger weather regimes. *J. Atmos. Sci.* **52**:3932–3944
- Orr WM. 1907. The stability or instability of the steady motions of a perfect fluid and of a viscous fluid. Part I. A perfect fluid. Part II A viscous fluid. *Proc. Roy. Irish Acad.* **27**:9–138
- Olvera D, Kerswell RR. 2017. Optimising energy growth as a tool for finding exact coherent structures. *Phys. Rev. Fluids* submitted
- Palmer T, Molteni F, Mureau R, Buizza R, Chapelet P, Tribbia J. 1993. Ensemble prediction. *Proc. ECMWF Seminar*. Reading, UK **1**:21–66
- Passaglia P-Y, Ehrenstein U. 2013. Adjoint based optimization and control of a separated boundary-layer flow. *Eur. J. Mech. B* **41**:169–177
- Peixinho J, Mullin T. 2007. Finite amplitude thresholds for transition in pipe flow. *J. Fluid Mech.* **582**:169–178
- Pralits JO, Hanifi A, Henningson DS. 2002. Adjoint-based optimization of steady suction for disturbance control in incompressible flows. *J. Fluid Mech.* **467**:129–161
- Pralits JO, Bottaro B, Cherubini S. 2015. Weakly nonlinear optimal perturbations. *J. Fluid Mech.* **785**:135–151
- Pringle CCT, Kerswell RR. 2010. Using nonlinear transient growth to construct the minimal seed for shear flow turbulence. *Phys. Rev. Lett.* **105**:154502
- Pringle CCT, Willis AP, Kerswell RR. 2012. Minimal seeds for shear flow turbulence: using nonlinear transient growth to touch the edge of chaos. *J. Fluid Mech.* **702**:415–443
- Pringle CCT, Willis AP, Kerswell RR. 2015. Fully localised nonlinear energy growth optimals in pipe flow. *Phys. Fluids* **27**:064102
- Rabin SME. 2013. A variational approach to determining nonlinear optimal perturbations and minimal seeds. *PhD thesis*, University of Cambridge
- Rabin SME, Caulfield CP, Kerswell RR. 2012. Variational identification of minimal seeds to trigger transition in plane Couette flow. *J. Fluid Mech.* **712**:244–272
- Rabin SME, Caulfield CP, Kerswell RR. 2014. Designing a more nonlinearly stable laminar flow via boundary manipulation. *J. Fluid Mech.* **738**:R1
- Rayleigh Lord. 1880. On the stability, or instability, of certain fluid motions. *Proc. London Math. Soc.* **11**:57–70
- Rayleigh Lord. 1916. On convection currents in a horizontal layer of fluid, when the higher temperature is on the under side. *Phil. Mag.* **6**:432–446
- Reddy SC, Henningson DS. 1993. Energy growth in viscous channel flows. *J. Fluid Mech.* **252**:209–238
- Reynolds O. 1883a. An experimental investigation of the circumstances which determine whether the motion of water shall be direct or sinuous and of the law of resistance in parallel channels. *Proc. R. Soc. Lond. Ser. A* **35**:84–99
- Reynolds O. 1883b. An experimental investigation of the circumstances which determine whether the motion of water shall be direct or sinuous and of the law of resistance in parallel channels. *Phil. Trans. R. Soc. Lond. Ser. A* **174**:935–982
- Schlichting H. 1955. *Boundary Layer Theory*. New York: McGraw-Hill
- Schmid PJ, Henningson DS. 1994. Optimal energy density growth in Hagen-Poiseuille flow. *J. Fluid Mech.* **277**:197–225
- Schmid PJ. 2007. Nonmodal Stability Theory *Ann. Rev. Fluid Mech.* **39**:129–62
- Schmid PJ, Henningson DS. 2001. *Stability and Transition in Shear Flows*. New York: Springer-Verlag
- Schneider TM, Eckhardt B, Yorke JA. 2007. Turbulence transition and the edge of chaos in pipe flow. *Phys. Rev. Lett.* **99**:034502
- Schneider TM, Gibson JF, Lagha M. 2008. Laminar-turbulent boundary in plane Couette flow. *Phys. Rev. E* **78**:037301

- Schneider TM, Eckhardt B. 2009. Edge states intermediate between laminar and turbulent dynamics in pipe flow. *Phil. Trans. R. Soc. A* **367**:577–587.
- Schneider TM, Gibson JF, Burke J. 2010. Snakes and ladders: localized solutions in plane Couette flow. *Phys. Rev. Lett.* **104**:104501.
- Taylor GI. 1923. Stability of a viscous liquid contained between two rotating cylinders. *Phil. Trans. Roy. Soc. Lond.* **223**:289–343
- Terwisscha van Scheltinga AD, Dijkstra HA. 2008. Conditional nonlinear optimal perturbations of the double-gyre ocean circulation *Nonlin. Processes Geophys.* **15**:727–734
- Thomson W (Lord Kelvin). 1887. Stability of fluid motion - rectilinear motion of viscous fluid between two parallel plates. *Philos. Mag.* **24**:188
- Trefethen LN, Trefethen AE, Reddy SC, Driscoll TA. 1993. Hydrodynamic stability without eigenvalues. *Science* **261**:578–584
- Wang Q, Mu M, Dijkstra HA. 2012. Application of the conditional nonlinear optimal perturbation method to the predictability study of the Kuroshio large meander. *Adv. Atmos. Sci.* **29**:118–134
- Wang Q, Mu M, Dijkstra HA. 2013. Effects of nonlinear physical processes on optimal error growth in predictability experiments of the Kuroshio large meander. *J. Geophys. Res.* **118**:6425–6436
- Wang J, Li Q, E W. 2015. Study of the instability of the Poiseuille flow using a thermodynamic formalism. *Proc. Nat. Acad. Sci.* **112**: 9518–9523
- Waugh IC, Juniper MP. 2011. Triggering in a thermoacoustic system with stochastic noise. *Int. J. Spray and Combustion Dynamics* **3**:225–242
- Willis AP. 2012. On the optimised magnetic dynamo. *Phys. Rev. Lett.* **109**:251101
- Yu YS, Duan WS, Xu H, Mu M. 2009. Dynamics of nonlinear error growth and season-dependent predictability of El Niño events in the Zebiak-Cane model. *Quart. J. Roy. Meteor. Soc.* **135**:2146–2160
- Ziqing ZU, Mu M, Dijkstra HA. 2013. Optimal nonlinear excitation of decadal variability of the North Atlantic thermohaline circulation. *Chinese J. Ocean. Limnology* **31**:1356–1362
- Zuccher S, Luchini P, Bottaro A. 2004. Algebraic growth in a Blasius boundary layer: optimal and robust control by mean suction in the nonlinear regime. *J. Fluid Mech.* **513**:135–160
- Zuccher S, Bottaro A, Luchini P. 2006. Algebraic growth in a Blasius boundary layer: Nonlinear optimal disturbances. *Eur. J. Mech. B* **25**:1–17